GIS BASED FLASH FLOOD HAZARD MAPPING AND SELECTION OF SUITABLE SITES FOR URBAN AGRICULTURE: THE CASE OF BISHOFTU CITY, ETHIOPIA

KUMERA GETU ASHENAFI

A THESIS SUBMITTED TO
THE DEPARTMENT OF WATER RESOURCES ENGINEERING
SCHOOL OF CIVIL ENGINEERING AND ARCHITECTURE

PRESENTED IN PARTIAL FULFILLMENT OF THE REQUIREMENTS FOR THE DEGREE OF MASTER'S IN WATER RESOURCES ENGINEERING (SPECIALIZATION IN IRRIGATION ENGINEERING)

OFFICE OF GRADUATE STUDIES
ADAMA SCIENCE AND TECHNOLOGY UNIVERSITY

June, 2023
ADAMA, ETHIOPIA

GIS Based Flash Flood Hazard Mapping and Selection of Suitable Sites for Urban Agriculture: The Case of Bishoftu City, Ethiopia

Kumera Getu Ashenafi

Advisor: Boja Mekonnin (PhD)

A Thesis Submitted To the Department of Water Resources Engineering
School of Civil Engineering and Architecture

Presented in Partial Fulfillment of the Requirements for the Degree of Master's in
Water Resources Engineering
(Specialization in Irrigation Engineering

Office of Graduate Studies
Adama Science and Technology University

June, 2023
Adama, Ethiopia

DECLARATION

I hereby declare that this Master's thesis, entitled “GIS Based Flash Flood Hazard Mapping and Selection of Suitable Sites for Urban Agriculture: The Case of Bishoftu City, Ethiopia" is my own work. It has not been submitted for the award of any academic degree, diploma, or certificate at any other university. All sources of material that were used for this thesis have been duly acknowledged through citation. It is being submitted for partial fulfillment for the award of the degree of Master of Science in Water Resources Engineering (Specialization in Irrigation Engineering) at Adama Science and Technology University School of Civil Engineering and Architecture.

Kumera Getu Ashenafi	______________________	_________________
Name of student	Signature	Date

RECOMMENDATION

I, the advisor of this thesis, hereby certify that I have read and evaluated this thesis entitled " GIS Based Flash Flood Hazard Mapping and Selection of Suitable Sites for Urban Agriculture: The Case of Bishoftu City, Ethiopia" prepared under my guidance by Kumera Getu Ashenafi and submitted in partial fulfillment of the requirements for the degree of Masters of Science in Water Resources Engineering (Specialization in Irrigation Engineering). Therefore, I recommend that the candidate has fulfilled the requirements and can submit the thesis to the department.

Boja Mekonnin (PhD)	______________________	_______________
Major Advisor	Signature	Date

APPROVAL PAGE

I, the advisor of the thesis entitled "GIS Based Flash Flood Hazard Mapping and Selection of Suitable Sites for Urban Agriculture: The Case of Bishoftu City, Ethiopia" and developed by Kumera Getu Ashenafi; hereby certify that the recommendation and suggestion made by board of examiners are appropriately incorporated into the final version of the thesis.

Boja Mekonnin (PhD)	____________________	________________
Major Advisor	Signature	Date

We, the undersigned, members of the Board of Examiners of the thesis by Kumera Getu Ashenafi have read and evaluated the thesis entitled "GIS Based Flash Flood Hazard Mapping and Selection of Suitable Sites for Urban Agriculture: The Case of Bishoftu City, Ethiopia and examined the candidate during the open defense. This is therefore, to certify that the thesis is accepted for partial fulfillment of the requirement of the degree of Master of Science in Water Resources Engineering (Specialization of Irrigation Engineering).

Mengistu Sime (PhD)	_________________	____________________
Chairperson	Signature	Date
Abdulkerim Bedewi (PhD)	__________________	____________________
Internal Examiner	Signature	Date
Habtamu Hailu (PhD)	____________________	____________________
External Examiner	Signature	Date

Final approval and acceptance of the thesis proposal is contingent upon submission of its final copy to the Office of Postgraduate Studies (OPGS) through the Department Graduate Council (DGC) and School Graduate Committee (SGC).

Department Head	Signature	Date
School Dean	Signature	Date
Office of Postgraduate Studies, Dean	Signature	Date

ACKNOWLEDGEMENTS

Above all, I want to thank the almighty God for providing me with health and energy to accomplish this work. Next, I kindly express my deepest gratitude to my beloved wife and children for their steadfast patience throughout the period of the accomplishment of this work. I would like to convey my heartfelt gratitude to my advisor, Boja Mekonnin (PhD); without him, my thesis would not have been a success.

I also wish my heartfelt gratitude to be extended to all my classmates, especially Tolosa Balemi, who has enlightened me during my entire career. I would like to thank Million Teshome for his moral support and motivation, as well as all my instructors for sharing their resourceful experiences and knowledge with me. Finally, there are colleagues whose names were not mentioned here but who made paramount contributions and cooperated with my work; I thank them once again.

TABLE OF CONTENTS

LIST OF TABLES

LIST OF FIGURES

LIST OF ACRONOMYS AND ABBRIVATIONS

AHP	Analytical Hierarchy Process
ALOS	Advanced Land Observing Satellite
CN	Curve Number
CSA	Central Statistical Agency
DEM	Digital Elevation Model
FFH	Flash Flood Hazard
GIS	Geographic Information Systems
LSM	Land suitability Map
LULC	Land Use Land Cover
MCE	Multi-Criteria Evaluation
MER	Main Ethiopian Rift
NMA	National Meteorological Agency
NPC	National Plan Commission
NWS	National Weather Service
PALSAR	Phased Array Type L-Band Synthetic Aperture Radar
RS	Remote Sensing
UA	Urban Agriculture
WBG	World Bank Group
WMO	World Metrological Organization

ABSTRACT

One of the most lethal natural disasters that affect human existence is the flash flood hazard (FFH). It occurs frequently, as soon as raindrops fall, and is followed by overflow, wrecking homes, destroying infrastructure, and killing living creatures. Although flash floods can happen anywhere on the planet, their effects are more pronounced in developing countries due to a lack of financial resources, a lack of skill to design and put in place drainage systems as per the design, poor housing options, insufficient early warning, and inadequate readiness. Hence, this study has been initiated to analyze and Map GIS-based flood inundation and locate suitable locations for urban agriculture (UA) by combining different factors that serve as flash flood resilience mechanisms and Selection of Suitable Sites for Urban Agriculture. Slope, drainage density, elevation, Curve Number, Rainfall, Land-use/cover classes, and Soil data were computed using Arc GIS software platforms. For the study, the Sentinel-2 satellite image, which has a 10-metre resolution, was used for LULC classification, while Slope, Elevation, and Drainage density data were generated from the 12.5-metre resolution of the ALOS Palsar DEM, and the rest of the factors were collected from the Ethiopian Metrological Institute. To create flash flood hazard zones (FFHs) and an appropriate land map for urban agriculture, all the data were regularized and merged using a GIS based on the analytic hierarchy process (AHP) technique. The FFH model revealed that Bishoftu City is classified as having four different levels of risk: very high (2106.4ha), high (10464.4ha), moderate (1444.44), and low (0.52), with respective percentages of 15.02%, 74.7%, 10.1%, and 0.004%. The results of the study showed that many residential areas in Bishoftu city, particularly the previously developed center, are vulnerable to flooding. Following similar methods and analysis procedures with FFH, the results of the urban agriculture land model revealed that four land Suitable Classes were identified: Highly Suitable (62.38%) (8765.8 ha), moderately suitable (0.02%) (2.8ha), currently not suitable (7.38%) (1037.6ha), and permanently not suitable (30.21%) (4245.5ha) this indicates that Bishoftu City is suitable for urban agriculture. In short, flood risk mapping is essential for raising public awareness of flood-prone areas, demonstrating susceptibility, strengthening financial capacity, protecting the environment, promoting environmental protection policy, and assisting first responders. Because Bishoftu is prone to flash floods, the municipality should priorities urban agriculture adaptation, proper settlement, and drainage network design.

***Key words**: Flash Floor, Urban Agriculture, Flood Mapping, Suitability Map*

1. INTRODUCTION

1.1 Background

The most frequent natural disasters that have an impact on societies worldwide are floods, which are thought to be a threat to more than one-third of the planet's surface area and 82 percent of its people (Argaz et al., 2019). One of the most harmful natural catastrophic dangers is FFH. It happens quickly, usually within an hour of rain, and is occasionally followed by mudslides, bridge collapses, building damage, and fatalities. It may occur everywhere, but its impacts are more pronounced in poorer nations because of a lack of financial resources, subpar housing options, insufficient warning systems, and a lack of readiness (El-Naqa and Jaber, 2018). About 40% of all natural disasters globally include flooding (Wakuma Abaya et al., 2009). Between 1950 and 2019, it posed a significant natural hazard in Africa, killing approximately 27, 000 people (Tramblay et al., 2020). Floods and droughts are the two natural disasters in Africa that have had the greatest humanitarian effects over the past 30 years based on the number of people impacted (Lumbroso, 2020). However, in terms of the number of people they affect, floods have surpassed drought in Africa during the past ten years (Legese et al., 2020). Large river basins, including the Congo, Niger, Nile, and Zambezi basins, are typically affected.

Disasters caused by climate change can exacerbate the socioeconomic and political circumstances that existed before the catastrophe, continuing a cycle of poverty and vulnerability (Amaratunga et al., 2019). According to studies, fast urbanisation would result in a larger accumulation of people, assets, and infrastructure; nevertheless, if such a situation is not adequately controlled and managed, it will result in increased problems and vulnerability to shocks and stressors (Charleson et al., 2017). Ethiopia's urban population is expected to nearly triple from 15 million in 2012 to 42 million in 2014, with an average annual growth rate of 5.4% (Ana Campos and Ankur, 2020). However, Ethiopian cities are dealing with access to jobs, infrastructure, services, and housing, as well as increased susceptibility to disasters and climate change impacts (Amaratunga et al., 2019).

However, in Ethiopia, understanding flood size estimation and management is still at an early stage. As a result, numerous homes and lives are routinely harmed in Jimma town (Feyissaa & Tufa, 2019). The extraordinary and abnormal magnitude of the floods is threatening several sections of the country. For instance, 357,000 people were affected by floods in 2006 (600 of whom died and 200,000 were left homeless), costing the government about 40 million Ethiopians (*Ethiopia: Dire Dawa Floods - OCHA Situation Report No. 2: Ethiopia | ReliefWeb*, 2023). The situation is especially serious in river basins and urban regions. Flooding in South Omo and Dire Dawa, for example, killed 300 people in Dire Dawa city in 2006. As a result, many people are impacted before the specific information is provided to the appropriate decision-makers (Garrison et al., 2007). Flooding has occurred in the South Omo Valley, Dire Dawa, Amhara, Afar, Somalia, Tigray, Gambella, and Oromia areas as a result of heavy rains across the country. According to official and United Nations (UN) data, roughly 35,000 people have been relocated, 120,000 have been affected, and 620 have been reported deceased. Flooding has remained one of the most severe natural disasters in the country, with only a few studies conducted, for example in Dire Dawa city, Oromia Region in Dugeda Bora Woreda; Addis Ababa; Gambella, Amhara Region in Fogera Woreda (Hagos et al., 2022).

Constantly expanding towns and cities, flooding challenge to development and people's lives in developing countries (Jha et al., 2012). Bishoftu is currently at risk for flash floods due to extreme climatic occurrences and its proximity to mountains; this risk is exacerbated by a poor drainage system, rapid housing growth, and the use of subpar building materials (Group, 2016). In Bishoftu, floods seem to be appearing more frequently and lasting longer. As a result, Bishoftu residents continue to worry about flooding.

Bishoftu city topography and landform are also undulating, with several ups and downs, rivers and streams (both perennial and permanent), swampy and crater lakes of Hora Harsedi, Babo Gaya, Kuriftu, Cheleleka, and Bishoftu, as well as associated mountain hills such as Gara Beru, Kidanemihret, and Sofa Mountain (Bayissa, 2022). The town's slope categorization reveals that the majority of the places discovered are flat areas, which are regarded as having severe drainage difficulties and being marshy and prone to flooding. Slope categories larger than 20% in the town, on the other hand, promote significant flash floods on the lower slopes in the down catchment. This means that the research region is especially vulnerable to flash floods caused by steep floods that settle on flat terrains.

According to Zhou et al.(2021), building resilient and sustainable cities is one of the pressing development challenges due to the increasing pressure of population growth as well as the adverse effects of climate change (Ebissa et al., 2023), and these challenges, including flooding risk damages, can be mitigated using urban agriculture. Urban agriculture reduces flood damage by shifting the economy from linear to circular (Deksissa et al., 2021a), replacing flood-prone areas (De Oliveira & Ahmed, 2021).

In general, the purpose of this research is to identify the key causes and impacts of the flash flood, as well as to develop flood maps of the Bishoftu city and selection of suitable sites for urban agriculture.

1.2 Statement of the Problem

Flooding is one of the most serious natural disasters in the world, causing deaths, infrastructural damage, and environmental degradation. Ethiopia is prone to flooding, which occurs at irregular intervals and varies in volume, duration, and impacted area (Mamo et al., 2019). In the last 50 years, both its frequency and size have drastically grown in emerging countries like Ethiopia, where population growth is fast and urbanization is less growing. People are highly vulnerable to disasters like floods, and the poor are more victimized because they live in hazard-prone areas. Disasters caused by nature occur worldwide, but their consequences are more severe in impoverished nations due to their poverty levels (Eleni et al., 2011). Flash floods are one of the natural hazards created by excessive rainfall in the upstream basin, which flows downstream with incredible concentration, velocity, and force. They are frequently unexpected and overlooked. As a result, such floods frequently take a great toll, and the damage becomes worse and more disastrous when they travel through or along human populations and infrastructure concentrations (Kebede, 2012). Floods are widespread in Ethiopian cities and towns, such as in Dire Dawa in 2006, which displaced 9,956 people and killed 256 (OCHA, 2006).

In Ethiopia, due to a smaller number of hydrological stations and stream gauging stations, the extent and characteristics of the Runoff are not well (Niekerk & Nemakonde, 2017). The natural topography and layout of Bishoftu is mostly the product of volcanic activity. Some of today's lakes are the product of geological formations. The Sofa, Baru, Bubissa, Dhibaayu, and Wulabbo mountains, which create a chain-like structure on the southern side of town, are major sources of flood water, causing damage in the town's center and periphery areas. The majority of the town's mountains are barren and vulnerable to natural disasters (Kumera & Woldetensae, 2023).

In flood-prone places, such as Bishoftu, developing mitigation strategies like UA might be an efficient way to capture extra runoff that is frequently lost and hence can be utilised during times of water scarcity (Yousif and Bubenzer, 2015). UA aids in increasing the quantity of water per unit cultivated area and improving groundwater levels (Sur et al., 2001), thereby aiding in the mitigation of water scarcity problems, particularly for agricultural and home applications (Li et al., 2000). As a result, developing a flood inundation map and planning urban agriculture is required.

1.3 Objective of the Study

1.3.1 General Objective

The main objective of this study was to develop flood inundation map and selection of suitable sites for urban agriculture by using GIS.

1.3.2 Specific Objectives

This research has the following specific objectives:

- To identify flood-causing variables and their contribution to flash hazard.
- To investigate the spatial distribution, areas, and estimation of flood depth.
- To develop a flood inundation map of Bishoftu city.
- To Estimate of Flush Flood depth and select appropriate area for Urban Agriculture

1.4 Research Questions

In line with the above objectives; the following research questions are designed to answer the established specific objectives:

- What are the primary contributing elements or causes of floods in the region?
- What is the spatial distribution of flash flood hazards in the study area?
- Which study areas are more susceptible to flood inundation?
- What are the appropriate sites for urban irrigated agriculture and how to estimate flood depth?

1.5 Significance of the Study

Understanding flood hazards during flood events and before they occur is critical for damage mitigation, resilience, and mitigation. Understanding flood risks, on the other hand, necessitates knowledge of the many forms of floods, their potential presence, and methods of modeling and mapping, needed data to generate hazard maps, and potential data sources. An in-depth comprehension of the flood hazards relevant to various regions is also essential in implementing suitable flood risk reduction strategies such as development planning, forecasting, and early warning systems (Sene, 2016). This effort will pave the way for bringing resilience to the study region through urban agriculture. Furthermore, this study will contribute a lot as a source for researchers who will conduct further studies in similar areas and with concerned government bodies.

1.6 Scope and Limitation of the study

Regarding the thematic focus of the study, a map of the flash flood hazard and selection of suitable sites for urban agriculture have been done for each area of Bishoftu city. It also assesses the possible impact of a natural hazard, as well as the primary causes and consequences of the flood, and proposes management tactics or local remedies that local communities might employ to reduce seasonal floods. Furthermore, the work builds urban flood danger maps utilizing various inputs, such as DEM files and geographical information.

1.7 Thesis Organization

This thesis study is organized into five chapters. The first chapter is the introduction, which contains the background, problem of the statement, objective of the study, research questions, significance of the study, and scope of the study. The second chapter is the literature review, which reviews articles and other necessary documents conducted on various thematic areas to fully address the topic of the study and easily understand it. The review includes a description of different topics and terminologies such as floods, flood hazards, flood mapping, flood-causing factors and their assessment, and flood modeling, and finally reviews studies on flood hazards. Materials and methods in the third chapter discussed the methodology from the data collection phase to flood hazard mapping and selection of suitable sites for urban agriculture. The fourth chapter describes the results of the study and discussion. Finally, the fifth chapter draws conclusions and makes recommendations based on the analysis of the results.

2. LITERATURE REVIEW

2.1 Floods and Floodplain

Flood is a branch of hydrology that is studied. It can be described as high-flowing water that rises and drowns out the normal dry surroundings (El-Naqa & Jaber, 2018). Flood zones are comparatively level alluvial terrain close to waterways that transport enormous amounts added water during flood events. When water reaches a place of flooding, it may threaten both the lives and personal assets of those who reside within or near the area of flooding (Alzahrani, 2017). Flood zones are frequently desired locations for people's activities and settlement, and they might offer comforts, hazards, and benefits. Natural resources and their uses are reduced during flooding. In the future, inhabitants on the floodplain will lose since the danger outweighs all of the benefits of residing on the floodplain (Shahpari et al., 2022).

2.1.1 Types of Floods

The categories of floods that are common and devastating in the watershed region have to be determined before conducting a risk and danger evaluation, because the techniques used for danger and risk evaluation vary based on the kind of flood. Many types of floods can be characterised based on the source of the water, the location of the receiving area, the cause, and the rate of onset(Shahpari et al., 2022b). Among the many varieties of flooding are river (fluvial) floods, pluvial floods (surface/overland), coastal (surge) floods, flash floods, and ice jam flooding. One of the most frequent types of flooding is a river flood, which usually happens when a river reaches its capacity because of extended periods of heavy rainfall (Khan & Sabbir, 2018). River floods pose a decreased chance of fatalities due to the slow rate of rising waters, giving people more time to take appropriate action(Gogoase et al., 2011). When surface runoff generation outpaces infiltration rates and drainage capacity, as frequently happens during high-intensity, brief storm rainfall events, pluvial floods result (Miller & Hutchins, 2017). Areas near the shore of a sea, an ocean, or any significant body of open water experience coastal flooding. It is brought on by a higher-than-average high tide and made worse by a lot of rain and onshore winds (wind coming from the ocean and blowing landward (Khan & Sabbir, 2018). When exceptionally heavy rain falls and the water can't be absorbed quickly enough. It can induce flash flooding, which is characterized by an intense, high-velocity torrent of water that happens in an existing river channel with little to no warning

(Davis, 2001). The creation of an ice jam causes a quick surge in water both at the jam's location and upstream, which is akin to flash flooding. A jam's failure causes unexpected flooding downstream. Failure of the jam results in sudden flooding downstream.

2.1.2 Causes of Flooding and Their Impacts

Worldwide, there are many different causes of floods, but why does flooding actually happen. Floods are the result of extreme hydro meteorological events, and the geometry of river basins, vegetation cover, and geomorphologic factors such as soil stability and permeability all affect how they develop (Khattak et al., 2016). Changes in land use, erosion and sedimentation, slums near rivers, inadequate flood control measures, heavy rainfall, river physiography, insufficient river capacity, the effects of high tides, land subsidence, water structures, and damage to flood control structures are all factors that contribute to floods. Water overflow is usually not a problem if it does not cause damage, fatalities, or injuries, does not linger in settlements for an extended period of time, and does not interfere with daily life in any other manner. Contrarily, if water pools at a high enough level and over an extended period of time, it will unavoidably make human activities more difficult (Sholihah et al., 2020). Floods can have devastating effects, including the loss of life for people and animals, the devastation of agricultural crops and land, the destruction of infrastructure and communication networks, and the transport of pollutants and sediment loads (Zoka et al., 2018).

2.1.3 Flood Hazard and Assessment

The term "flood hazard" refers to the possibility of potentially damaging flood events occurring in a certain location and time period (Prinos et al., 2008). The goal of analysing flood hazards is to determine the likelihood that a flood will be more severe than a specific limit over a lengthy period of time. It necessitates determining the features of each flood as well as their probability of occurring. A map of flood dangers displays flood characteristics for a specific return time. Flood frequency (the likelihood of an occurrence in a given time period), extent (the area affected), severity (intensity, water level or depths), flow velocity and/or direction, and duration of inundation (the amount of time an area will or may have been under water) are some of the characteristics of floods (Benito & Hudson, 2010). The map delineates flood hazard zones and generates quickly accessible charts and maps that are simple to read and understand, making it easier for policy makers and planners to detect hazard areas and rank their mitigations (Chakraborty & Biswas, 2020). It can be used to make sure that preparation, response, and recovery are effectively carried out to lessen the effects of flooding (Ekeu-wei & Blackburn, 2018). Vertical aerial pictures are one instrument that can be used to create a flood hazard map. Agents can assess the cost-effectiveness of flood control measures using flood risk evaluations, and they can also notify citizens, insurance providers, and municipalities about the risks so they can plan for disasters (Shah et al., 2018). This is critical for the design and operation of flood control structures (dams, retaining basins), infrastructure objects (flood defences, bridges, roads, and dams), as well as flood risk management, planning, flood risk mapping, and the improvement of alert methods within a region (Leščešen & Dolinaj, 2019).

2.1.4 Flood Mapping: Process and Products

Flood mapping is both a technical and administrative endeavour. The examination of numerous data and characteristics indicating flood conditions (previous floods, flood forecast) in a flood plain, encompassing a whole river basin, along a single river reach, or on an alluvial fan is known as flood assessment. Flood mapping specifically refers to the creation of flood maps, whereas flood assessment implicitly includes this process. Similar considerations are made for the areas on alluvial fans, that could be impacted by mud or debris flow utilizing new information on sediments and sediment movement (Gwam, 2010)

Maps used in the flood management process, such as flood risk maps, flood hazard maps, and others, frequently show the findings of a flood assessment conducted in a specific location. Different stages of flood assessment are known depending on the goal: The most typical flood evaluations are preliminary and detailed; occasionally, a general-purpose assessment is utilized as a transitional stage. One or more methodologies (historical, geomorphic, or modelling) are used at each of these stages. The numerous facets of flood assessment will be highlighted in the sections that follow: The flood mapping procedure is described, and the results are shown in the final two parts.

2.2 Determination of Flood Magnitude

Flood estimate approaches try to predict rainfall-runoff connections and are classified into three types based on their complexity. The rational technique and empirical formulae, for example, estimation of the peak discharge quickly and with a small number of inputs. A humble flood estimation approach is the Curve Number (CN). Detailed or complicated models, as opposed to presenting a basic representation of general conditions, can pinpoint the origins of issues (Mihalik, 2007). In engineering design and flood control projects, notably in the United States, the CN technique is widely used (Storey et al., 2009). GIS and RS approaches have been used to determine flood risk (Yousif & Bubenzer, 2015). Additionally, GIS model that combines an inundation model and a storm-runoff model to simulate flood threats. Additionally, a GIS batch procedure was built to define catchments and determine their geomorphologic properties. Additionally, it has investigated the flood features and changes of significant basins in India using a variety of data sources and two runoff models in a GIS platform. GIS was also used to create inundation maps for extreme flood events. Moreover, Gogoase et al., (2011), created inundation maps for severe flood periods using GIS.

2.3 Analytical Hierarchy Process

In the Analytical Hierarchy Process (AHP), weights and thematic layers of each level (criteria classes) are assigned, and their relative importance is calculated using Saaty's 1–9 scale. The importance of each theme layer in relation to the other thematic levels on flood-prone region delineation and selection has been expressed by assigning weights. This has been performed by using associated review literature, field observation, and expert opinion to populate a pairwise comparison matrix from which Eigenvectors and consistency ratios can be calculated. From there, consistency ratios and a set of weights known as Eigenvectors will be generated for each of the criteria being taken into consideration. On a scale of 1 to 9, flood hazard factors are ranked, with 1 denoting equal importance for both elements and 9 denoting greater importance for one aspect. According to Saaty & Vargas, (1991), the reciprocal of 1 to 9 (1/1 and 1/9) indicates that one is less significant than the other. The factor weights will be assessed in a study region in order to undertake a multi-criteria assessment of the impact on flood generation.

The AHP, a multi-criteria decision-making approach, was used to rank and weight the sub-factors and map layers according to their effect on the outcome. Before the final resultant map is generated and categorised based on the food hazard model's recommendation, these layers will be subjected to a weight overlay analysis.

2.4 Urban Agriculture as a Strategy for Building Water Resilient City

Growing or producing food in urban areas is known as urban agriculture (Baker, 2016). Urban flooding is a phenomenon that develops as a result of ongoing land-use changes that produce impervious surfaces (Lucertini & Di Giustino, 2021). It has a negative impact on people's lives and property, particularly compromising cities' resilience and sustainability (SDG 11). The Sustainable Development Goals (SDGs) are a call from the United Nations (UN) to achieve a healthy world by 2030 through the implementation of 17 goals, five of which are relevant to this proposal (zero hunger, good health and well-being, clean water and sanitation, sustainable cities and communities, and climate action). Ending hunger and malnutrition by 2030 is expected to be accomplished through the promotion of sustainable agriculture, the assistance of small-scale farmers, the promotion of fair access to land, and the expansion of technologies and markets.

2.4.1 UA for creating a circular water economy

The need for integration was prompted by the fact that the various land-use types in urban areas are currently planned and handled individually or separately (Bettencourt & West, 2010), which has increased the vulnerability of urban areas to risks (Cai et al., 2021) and their reliance on surrounding communities or rural areas for the provision of ecosystem services (Sukhwani & Shaw, 2020). Changing from a linear to a circular economy is essentially what happens when diverse land-use types are integrated to improve a city's ecosystem services. In order to overcome obstacles and improve ecosystem services and the economic sector, urban agriculture (UA) and urban storm water management must be integrated(Deksissa et al., 2021c). According to (Langemeyer et al., 2021). UA solves sewer overflow while also supplying food and fiber; as a result, UA is essential for creating circular economies and cities (Deksissa et al., 2021).

2.4.2 Allocating flood-prone areas

Flooding occurrences increased by 50% globally in the previous decade, according to UA studies (Steenkamp et al., 2021), and cities have thus designated flood-prone regions for UA as a strategy for managing flooding hazards. However, before designating flood-prone regions for any use, it is suggested that an environmental impact study be performed. While flood-prone regions are designated for UA as a risk-mitigation approach, existing and functional UA also serves as a buffer zone during floods. According to research from Ghana (de Oliveira & Ahmed, 2021), flood-prone and low-lying valleys were designated for urban agriculture.

2.4.3 UA acting as a buffer zone

A buffer zone is a location set aside to guard against flooding risks that could harm a resource or a city and its citizens. The existence of a buffer zone in an urban region has positive effects on the environment, society, and the individual yet it is difficult to measure these effects in practice (Vejre et al., 2010). From an environmental standpoint, the buffer zone serves to prevent flooding, preserve biodiversity, and protect environmentally sensitive areas from damage, while the socio-economic advantages of tourism activity and its resource use are accounted for by (Kim et al., 2012).

2.4.4 UA as infiltration enhancer

Infiltration is the downward entrance of water into the soil stated in inches per hour, which is critical to hydrological knowledge (Beven et al., 2021) and is influenced by hydrologic soil types or groups. The USDA (United States Department of Agriculture) classified soils into four kinds based on their infiltration capability, which ranged from poor to high (Hoeft, 2020). According to Hoeft (2020), curve number (CN) is an empirical quantity used to forecast direct infiltration or runoff from surplus rainfall or a method for predicting runoff depth from rainfall depth (Soulis, 2021). The value of CN ranges from 0 to 100 with a lower number suggesting strong infiltration and a higher number indicating low infiltration or high run-off potential (Erdinata et al., 2021).

2.4.5 UA as a nature-based solution against flood risks

As climate change intensifies, the repercussions of floods, particularly in vulnerable places, will be jeopardized (Shao et al., 2021), and nature-based solutions are seen as natural insurance against flood risks in vulnerable areas (Zandersen et al., 2021). Insurance capacity is the value of ecosystem services in mitigating external disruption and, as a result, lowering risks to people and infrastructure (Zandersen et al., 2021). As a result, cropland can be employed as intentional inundation receptors to safeguard fragile and important metropolitan assets downstream.

2.4.6 Flood harvesting

Climate change is increasing UA water demand, where storms may be caught for use in the system while also being used to mitigate urban flooding hazards (Liu et al., 2021). Accordingly, Deksissa et al. (2021), provide practical examples of reservoirs built on the Karun River in Iran that are used to meet water requirements for agricultural, industrial, domestic, and environmental demands with pre- and post-release capacities equal to, half of, or equal to the reservoir capacity. According to a study of 100 small urban farmers in Nigeria, irrigation water in Lagos comes from shallow wells that flood during rainy seasons. The use of blue-green roofs to collect rainwater for later use and thereby mitigate flooding impacts has gained a lot of attention. According to Busker et al. (2022), blue-green roofs may absorb between 70% and 97% of heavy precipitation of more than 20 mm/h, which is much higher than the 12% capture rate of a standard green roof without additional water retention. Extra water is rainwater captured by blue-green roofs via an automated valve that drains extra water during extreme precipitation, which is absent from conventional green roofs; or simply, extra water is the difference in the amount of water captured by blue-green roofs and conventional green roofs (Busker et al., 2022).

2.5 CROPWAT model

Using crop and climate data, CROPWAT is computer software that determines irrigation, reference evapotranspiration, and crop water needs. The application also enables the creation of irrigation schedules for various management scenarios and the estimation of scheme water supply for various agricultural patterns. Any IBM-PC-style computer with a minimum memory size of 360Kb may execute the application (FAO, 1992). One of the models created by Smith (1991) of the Food and Agricultural Organization (FAO) and widely utilized in the field of water management worldwide is CROPWAT. (George *et al*; 2000) claim that CROPWAT makes it simpler to calculate irrigation schedules, crop water requirements, and evapotranspiration for various cropping patterns. The decision support tool CROPWAT was developed by the FAO's Land and Water Development Division to aid in the management and planning of irrigation systems. It makes it possible to plan irrigations under various water supply scenarios, come up with ideas for better irrigation methods, and assess production in rain-fed or shortfall irrigation settings. (FAO 1992).

3. MATERIALS AND METHODS

3.1 Study Area

3.1.1 Location and Topography

Bishoftu city is located in the east Shoa zone of Oromia regional state in Ada woreda (district), about 46 Km southeast of Addis Abeba, with central coordinates of 8° 44′ 5″ to 8° 45′ 0″ N latitude and 38° 59′ 0″ to 39° 0′ 30″ E longitude, as shown in Figure (3.1).

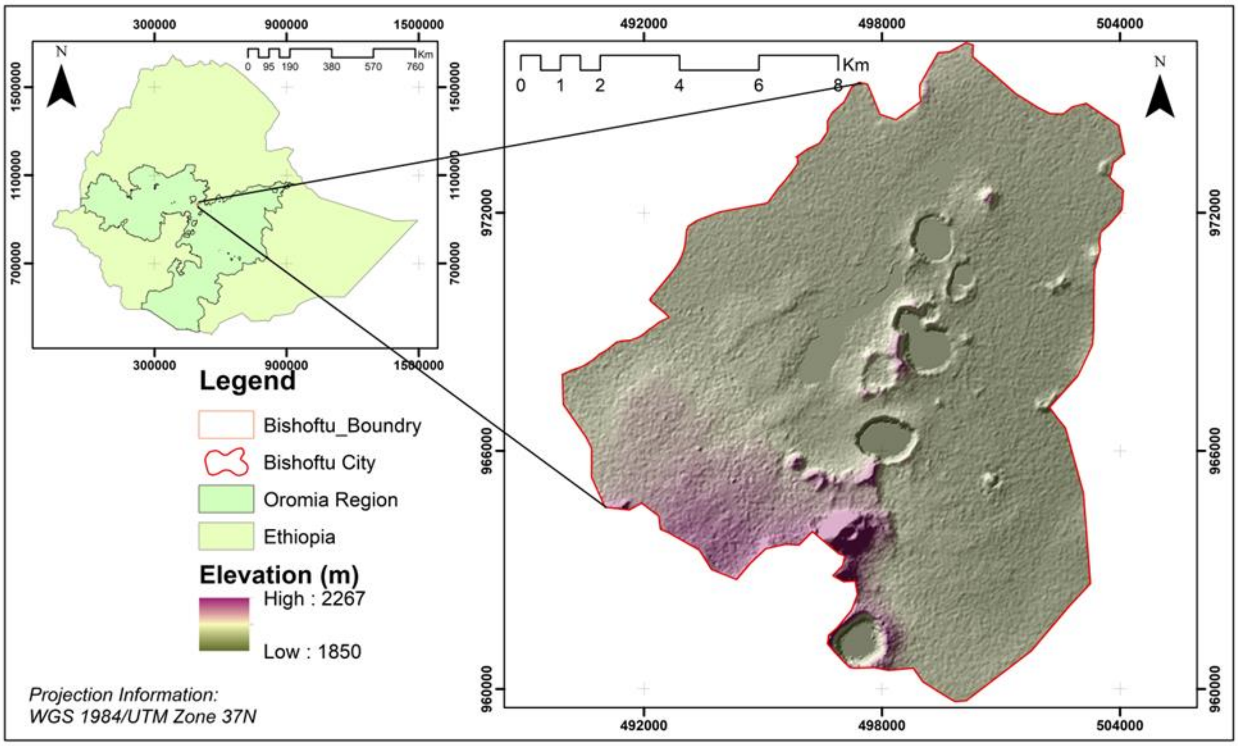

Figure 3:1 Map of the study's area

3.1.2 Demography

Bishoftu city is a Woreda administrative centre; however, it is the fourth largest urban centre in the Oromia Region in terms of population size, after Adama, Jimma, and Sashemene, and one of the few towns in the country with a population threshold of around 207,383. The district divisions given here are based on the 2007 census atlas and current government forecasts. Actually, the number of districts and townships is greater. Several boundaries have also shifted since then. Because of the presence of many lakes, vast military camps, many research and educational institutions, industrial establishments, and developed urban agriculture within the city, Bishoftu is quickly becoming one of the largest urban centres in the Oromia region; its area is thought to be much larger than implied by its population size.

3.1.3 Climate

According to the Ethiopian Traditional climatic zone categorization, locations between 1500 and 2300 meters in elevation are classified as Woyna Dega agro-climatic zone (Deressa et al., 2010), Dega since its elevation ranges from 1835 to 2359 meters. The town's average annual rainfall and temperature figures, on the other hand, are 860mm and 19.32 °C, respectively.

3.1.4 Topography

Bishoftu city is located at an elevation of 1850m to 2267m above sea level (Figure 3.1). As a result, the town has an average elevation of 2058m above sea level. The geography of Bishoftu city and its environs is typically described as extensive plain regions, marshy and water bodies, soft, rounded hips and high mountains, sharp and rounded hills, and accompanying undulating dissected areas (Bayissa, 2022). The southern half of town is related to and characterised by undulating and mountainous terrain, but the eastern section is mostly flat. In terms of area coverage, flat lands, on the other hand, formed the biggest amount. These locations may be found in the expansion directions of the east, north, and west. The soft, rounded hips seen in the town centre were noted to be accessible by both non-motorised and motorised means of transportation.

Due to the possibility of rapid runoff, the slope is a key component of flash flooding risk. Experience has shown that any slope greater than 30 degrees causes’ exceptionally fast runoff and a prompt reaction in local creeks and streams. Whereas slopes ranging from 0-2% typically have drainage issues, such places are also particularly prone to flooding. Bishoftu's topography and landform are also undulating, including various ups and downs, rivers and streams (both perennial and permanent), marshy and crater lakes like Hora Harsedi, Babo Gaya, Kuriftu, Cheleleka, and Bishoftu, and adjacent mountain slopes such as Gara Beru, Kidanemihret, and Sofa Mountain (Bayissa, 2022).

3.1.5 Geology

According to Abebe et al. (1998) the geology of the Main Ethiopian Rift (MER), which includes the study region, is dominated by Quaternary Volcanic layers underlain by Tertiary and Late Tertiary volcanic rocks and, in certain areas, Sedimentary rocks. The volcanic rocks are mostly basaltic lava flows and central-type volcanoes that are restricted to the top half of the succession. From the Miocene to the Pleistocene, eruptions generated consecutive strata with almost identical composition. The Bishoftu region is located between the Ethiopian Plateau and the Main Ethiopian Rift (MER). The rift escarpment is poorly defined in this location, and the MER contacts a major E-W structure (the Yerer-Tullu Wellel Volcano Tectonic Lineament). The layers of the Bishoftu region are rarely exposed, in addition to the several volcanic hills and crater cones. There are few outcrops of lacustrine sediment deposition in the plain areas. The lacustrine deposits are largely composed of redeposited volcanic sands, calcareous tuff, and diatomite. The area is dominated by volcanic rocks, with sedimentary rocks consisting of an alluvial cover and lacustrine phases. The area's volcanic activity has produced core composite volcanoes as well as monogenic strata like domes, spatter cones, and maars (Feyissaa & Tufa, 2019).

3.1.6. Soil

As previously stated, the geography of the Bishoftu region ranges from virtually flat to undulating, with some hills and ancient volcanic cones thrown in for good measure. The geographic location of a Bishoftu city, the type of parent material from which the soil came, and other variables can all influence soil properties. As a result, the soil in the Bishoftu area might be a weathered product of the volcanic rock that formed the location as well as an alluvial kind that was held down from the surrounding hills and deposited on the lower-level surface. The soil around Bishoftu consists mostly of grey to extremely black clays or clay loams. In addition, in some areas, there are also brown to reddish-brown clay soils. On the other hand, the slope of the hills is often reddish brown, and in the lower areas, the soils are dark.

In general, the Bishoftu soil type is defined as black clay and extremely dark grey clay with a high organic content, with this type of soil character having a strong potential for agricultural output. However, such soil has a significant swelling and shrinkage characteristic, which makes it unsuitable for building and development; thus, careful thought must be given before any form of development. Such soil characteristics often have a poor infiltration rate after heavy rains and facilitate fast runoff (Lillesand et al., 2015)

3.2 Tools and Software Programs Used

As the study is about urban expansion, spatial patterns, and landscape dynamics measurement, mainly ENVI 5.3 and ArcGIS 10.8 software program were used for data processing, and flood hazard mapping was added to the land suitability analysis in this study. ENVI is important software for image preprocessing, enhancement, transformation, classification, and accuracy assessment activities. Whereas ArcGIS software was applied for analysis, flood hazards mapping, and urban agriculture land suitability analysis and also CropWat 8.0 was used for determine crop water requirements.

3.3 Methods

3.3.1 Material Used for Data Collection

The quality of the geographic data utilised determines the effectiveness of any GIS application. Collecting high-quality geographic data for GIS input is thus a vital stage. Data gathering is one of the most time-consuming and expensive aspects of GIS-based research. GIS can store a wide range of geographic data types originating from a number of sources. Primary and secondary raster and vector data were employed in this investigation. The examination of satellite pictures yielded primary data. Secondary data was gathered from both public and unpublished sources, such as books, journals, research articles, and census records. Secondary data was gathered from a variety of sources. Previous research studies in the study area bordered on data from the Central Statistical Agency (CSA) that provided background information on the study regions. The National Meteorological Institute (NMI) provided rainfall and temperature data. The digital elevation model, soil classification, Sentinel-2 satellite photos, rainfall, drainage density, and administrative boundary shapefiles are all significant data for this investigation. ENVI 5.3 was used to extract land-use and land-cover data from Sentinel-2 pictures.

3.3.2 Satellite imagery

Remote sensing imagery is the most common kind of main raster data source since it is popular. As a result, in order to derive Land-use and land-cover categories, to identify the land use and land cover of the research region, a cloud-free, 10-metre-resolution Sentinel-2 picture collected in January 2023 during the dry season was studied. ENVI 5.3 was used for geometric correction and picture enhancement.

3.4 Data Analyses

3.4.1 Image classification

With the improvement of technological applications, great effort has been made to develop a better-automated platform for image classification algorithms. In contrast to the visual interpretation approaches, where knowledge of a whole landscape is needed, automated classification approaches only need samples from the site as training inputs (Lelsand et al., 2015). For this study, a supervised classification approach was applied, which is based on the analyst's understanding to acquire sets of training samples, and then an image classifier was applied to distinguish the LULC label for each pixel in the remotely sensed images (Ayhan & Kansu, 2012) using ENVI 5.3 software. The study has applied a Support Vector Machine (SVM) classifier, which is a kernel-based algorithm where the training data is initially scaled, upon which a discriminant utility is used (Mountrakis et al., 2011). Because it needs a small sample size, global optimizations, and ease of use (Cao et al., 2019). The study thereby categorized five land cover types: (a) agricultural land; (b) Built-up area; (c) vegetation cover; (d) bare land; and (e) water body. They were classified based on the spectrum responses of features on Sentinel-2 photos, local knowledge, visual examination of various remote sensing products, and usage of higher spatial resolution imaging. Table (3.1) describes the various land-use/cover classifications.

Table 3:1 Classes and descriptions of land use/cover (LULC)

LULC Classes	**Description**
Urban/built-up areas:	Commercial, Residential, transportation, industrial, services, communication and utilities.
Agricultural areas:	Cropland, horticultural farms, irrigation farms and other agricultural crops.
Vegetation cover:	Land covered by forest patches, woodland, shrubs, scattered trees mixed with grass, and perennial crops.
Water bodies:	Lakes, rivers, and ponds.

Bare land:	Rocks, bare soil, etc.

3.4.2 Analysis of Classification Accuracy

Land-cover maps created from remote sensing images usually contain errors due to a variety of reasons, ranging from the categorization approach to the satellite data gathering method. The creation of a classification error matrix or a confusion matrix is one of the most frequent ways of showing classification accuracy (Lillesand et al., 2015). Because each category is clearly specified, it is a particularly effective approach to communicating accuracy. Most of the assessments used the same data set that was used to train the classifier. Congalton (1991) discovered that using the same data set for training and testing resulted in an overestimation of classification accuracy. The accuracy of the producer is determined by dividing the total number of accurate pixels in a category by the total number of pixels in that category generated from the reference data (i.e., the column total). This accuracy value represents the likelihood of a reference pixel being properly classified. In contrast, user accuracy or dependability is defined as the total number of accurate pixels in a category divided by the total number of pixels classified in that category.

For accuracy evaluations, 2500 points of ground truth data were collected from high-resolution Google Earth pictures in the current study. Additionally, critical accuracy evaluation components such as the error matrix, user and producer accuracies, and kappa coefficient were generated. The WGS 1984 and UTM Zone 37 projection systems are utilised to geo-reference all datasets in this assessment..

3.5 Mapping of Flash Flood Hazards

The most difficult aspect of multi-criteria evaluation (MCE) is identifying to incorporate information from several criteria to develop a single assessment index. A set of basic maps and pictures was developed to help in the processing, data integration, and operation of geographical information system (Eastman, 2006).Before analysis, all preparatory operations, such as downloading, extracting, geo-referencing, formatting, and resampling digital data from the factors, were accomplished. Field surveys and the literature were utilised to identify flood-causing factors.

All of the factor layers are ready to be integrated at the data analysis step to estimate the flood hazard zones in the research region. If all datasets were equally relevant, they may be simple to merge. However, the relative relevance of each parameter was assessed using the primary eigenvector method. As a result, the greater the weight, the greater the effect a given element will have on flood generation. As a result, the factor layers were generated in QGIS 4.2 using the Full Multi criteria Evaluation plugin extension. This plugin provides comprehensive multi criteria evaluation (MCE) tool for vector data. It supports reclassifying constraints to Boolean, normalizing factors to obtain the weight of each component via a pairwise comparison matrix, and combining constraints and weighted factors using Weighted Linear Combination (WLC).

Mapping Flood Hazards Based on current reality and knowledge of the study region, the main causal variables for the occurrence of flooding hazards in the study area were determined. Bishoftu city flood hazard study was performed utilizing weighted sum overlay analysis of the seven reclassified flood causative elements (i.e., rainfall, drainage density, slope, elevation, curve number, soil, and land-use/land-cover Layers) added.

Three key stages were used to map flood danger areas: First, the criteria maps were standardized/reclassified using the Reclassify function in Spatial Analyst. This phase is required since the criterion maps include ordinal values (very high, high, moderate, low, and very low) indicating the degree of flood threat for a certain criterion (criteria standardization). Second, the pairwise comparison approach was used to derive the relative relevance criteria. Once the pairwise comparison matrix is inserted in the Full Multi-criteria Evaluation plugin extension in the QGIS weight derivation module, the criterion weights are automatically produced.

Third, using weighted overlay approach analysis, the criteria weights and standardized criterion maps were combined/ aggregated. The criteria for flood danger zones in Bishoftu city are shown in Table (3.2).

Table 3:2 Flood Hazard Mapping main causes of flooding

Criterion	Very High	High	Moderate	Low	Very Low
Slope (Degree)	0-8	8-15	15-30	>30	
Drainage	0.02-1	1-2.5	2.5-4.5	4.5-6.5	6.5-11

(Km/Sq.Km)					
Elevation (m)	1850-1888	1888-1924	1924-1974	1974-2068	2068-2,267
Rainfall (mm)	600-800	400-600, >80	250-400	>50	
Soil (Texture)		Sandy Loam		Clay	
Curve Number	92-100	88-89	82-83	67-77	*43-65*
Land-use/ land-cover	*Built-up area*	Bare Land	Agriculture land	Vegetation Area	*Water body*

3.5.1 Slope

Slope was created using ALOS PALSAR data in the GIS platform for the current study, utilizing the Geostatistical Analyst's surface analysis approach. The slope map of the research region is depicted in Figure 3.2.. The slope raster was created from the digital elevation model using the ArcGIS Spatial Analyst extension of the surface module, which allowed the region to be classified according to the steepness and roughness of the terrain. The greatest rate of change between each cell and its neighbors might be calculated using the Slope function. A slope value was assigned to each cell in the output raster. The flatter the terrain, the lower the slope value, and the steeper the terrain have the greater the slope value.

During floods, the low-lying area with a low slope angle has been swamped first, followed by the high-slope sector. The steep slope sections have a higher peak discharge than the low parts, causing the storage in the upstream areas to be depleted. The slope raster was then subdivided into five subgroups using natural breaks. The reclassified slope was assigned a value ranging from 1 to 5, with a higher value of 1 suggesting a strong influence, leading to a very high flood rate, and a lower value of 5 indicating very little influence. The reclassified slope was assigned a value between 1 and 5, with 1 indicating high influence and a very high flood rate and 5 indicating very low influence and a very low flood rate. Table 3.2 contains the slope classes. This method provided a higher flash flood hazard to slope classes with lower degrees.

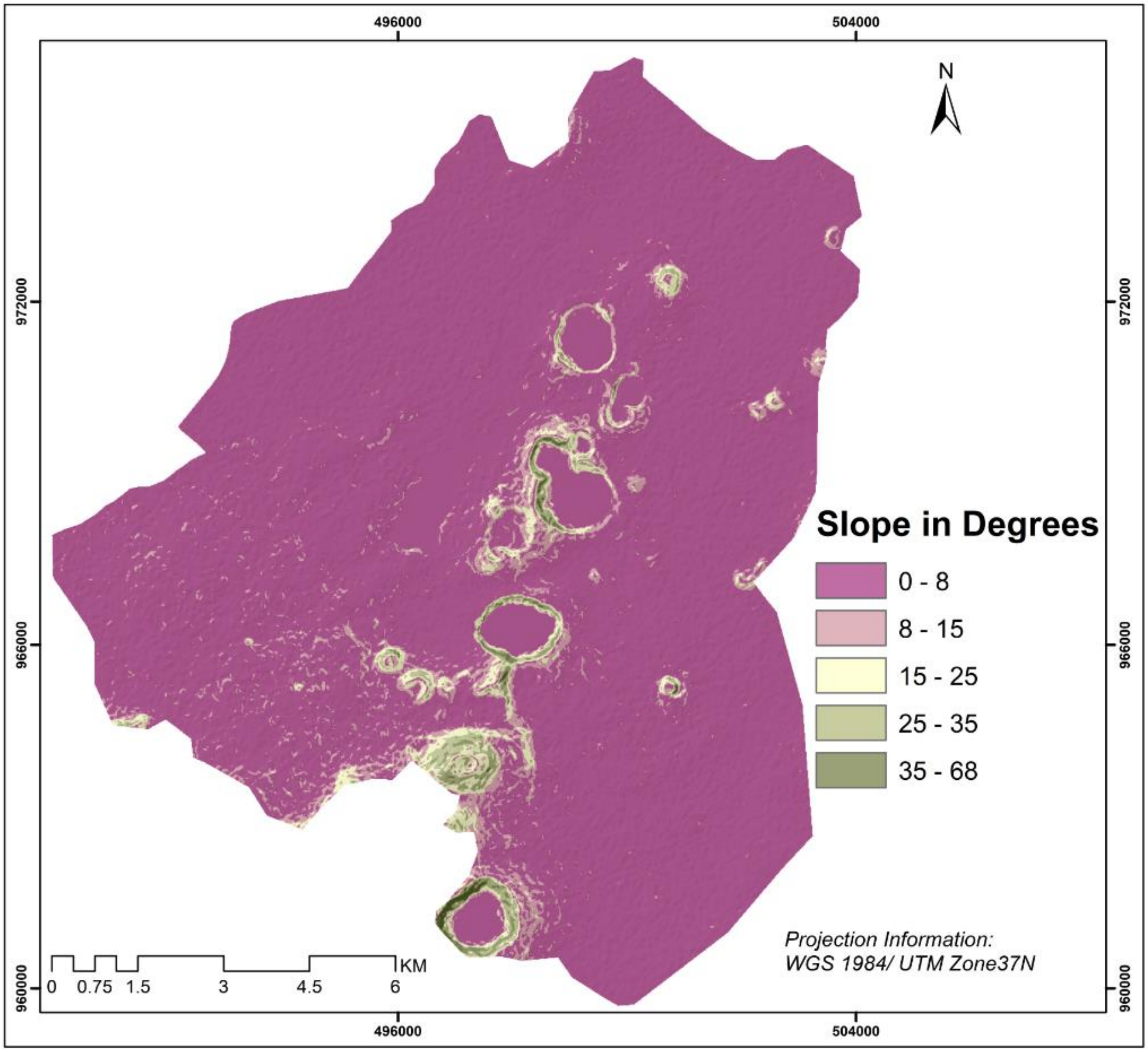

Figure 3:2 Slope Map of Bishoftu City.

3.5.2 Drainage Density

The density of drainage is a major factor influencing flood hazards, and it is an inverse function of soil permeability. Rainwater creates excessive runoff, and vice versa when there is a low permeable surface area. As a result, increased drainage density means less flooding in the region (Wondim, 2016). The drainage networks were built in ArcGIS 10.8 using a spatial analysis tool and DEMs with a resolution of 12.5 m. In a GIS setting, Line Density was utilised to measure drainage density areas utilising stream polyline features. Line Density was employed in a GIS context to evaluate drainage density areas using stream polyline data, as shown in Figure 3.3.

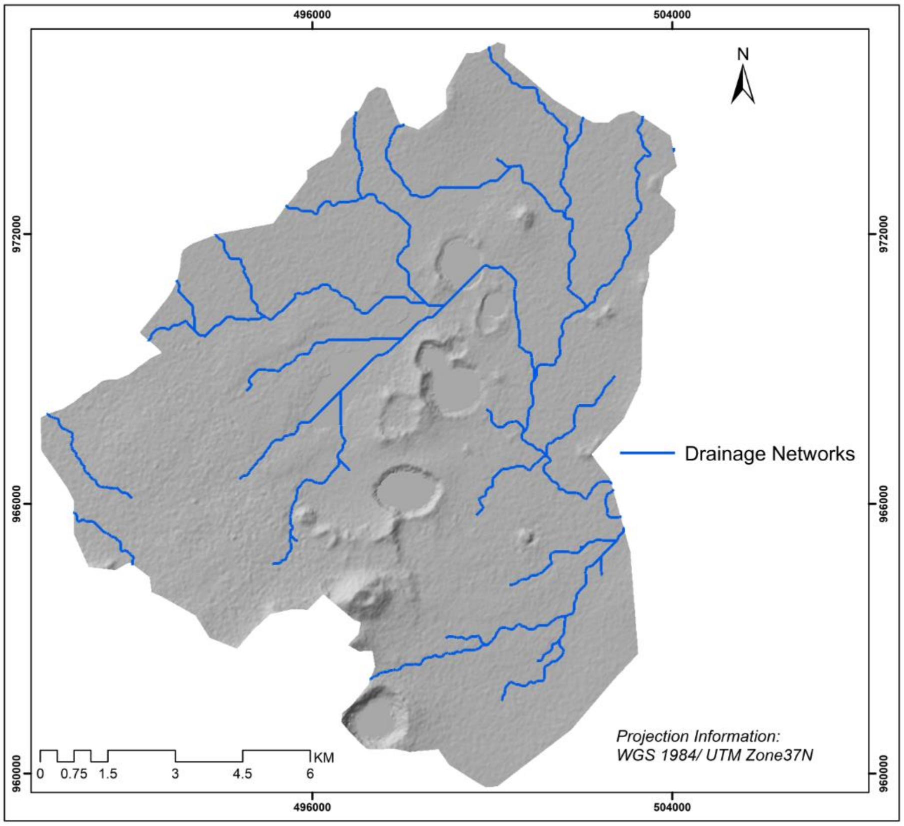

Figure 3:3.3 Drainage Network of Bishoftu City

The drainage density was determined by dividing the total length of all rivers and streams in a drainage basin by the total area of drainage (Gazi et al., 2019)

$$\mathrm{Dd} = \frac{\sum_{i=1}^{n} L_i}{A} \qquad 3.1$$

Where, ‘Li’ is the length of drainage in Km,

‘A’ is total area of study site in Km^2, and

‘n’ is stands for number of drainage networks in the watershed.

Generally, the drainage density was classed into a continuous scale in accordance with the flood hazard. As indicated in Figure (3.4), the produced drainage density in the city was divided into five classes ranging from 0.002 to 10.97 $\mathrm{km/km}^2$.

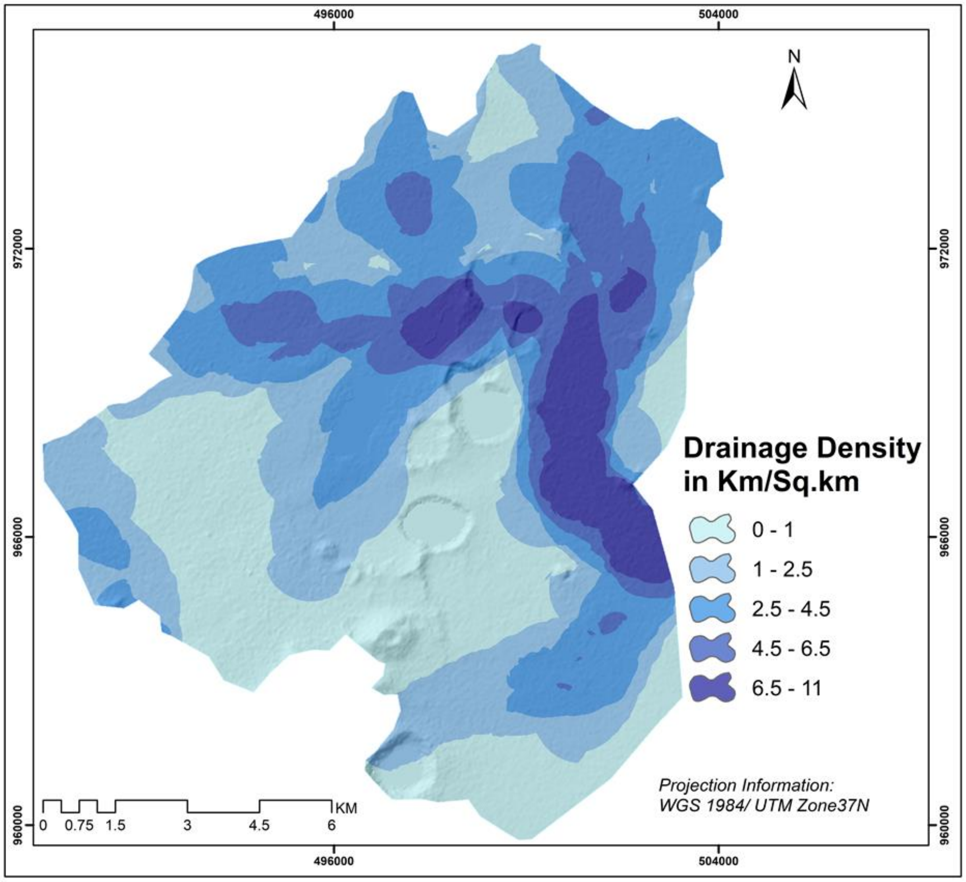

Figure 3:4 Drainage Density of Bishoftu City.

3.5.3 Elevation

The raster elevation was created in a GIS context using a 3D analyst tool from a filled DEM with a resolution of 12.5 m. Elevation values were included in the final raster. The elevation was then categorised into five distinct elevation groups based on its impact on flood risk. According to their flooding susceptibility, the lower the elevation value, the greater the flood hazard, and the higher the elevation value, the lower the flood hazard. The elevation classes' rank and level of hazard are depicted in Figure (3.5).

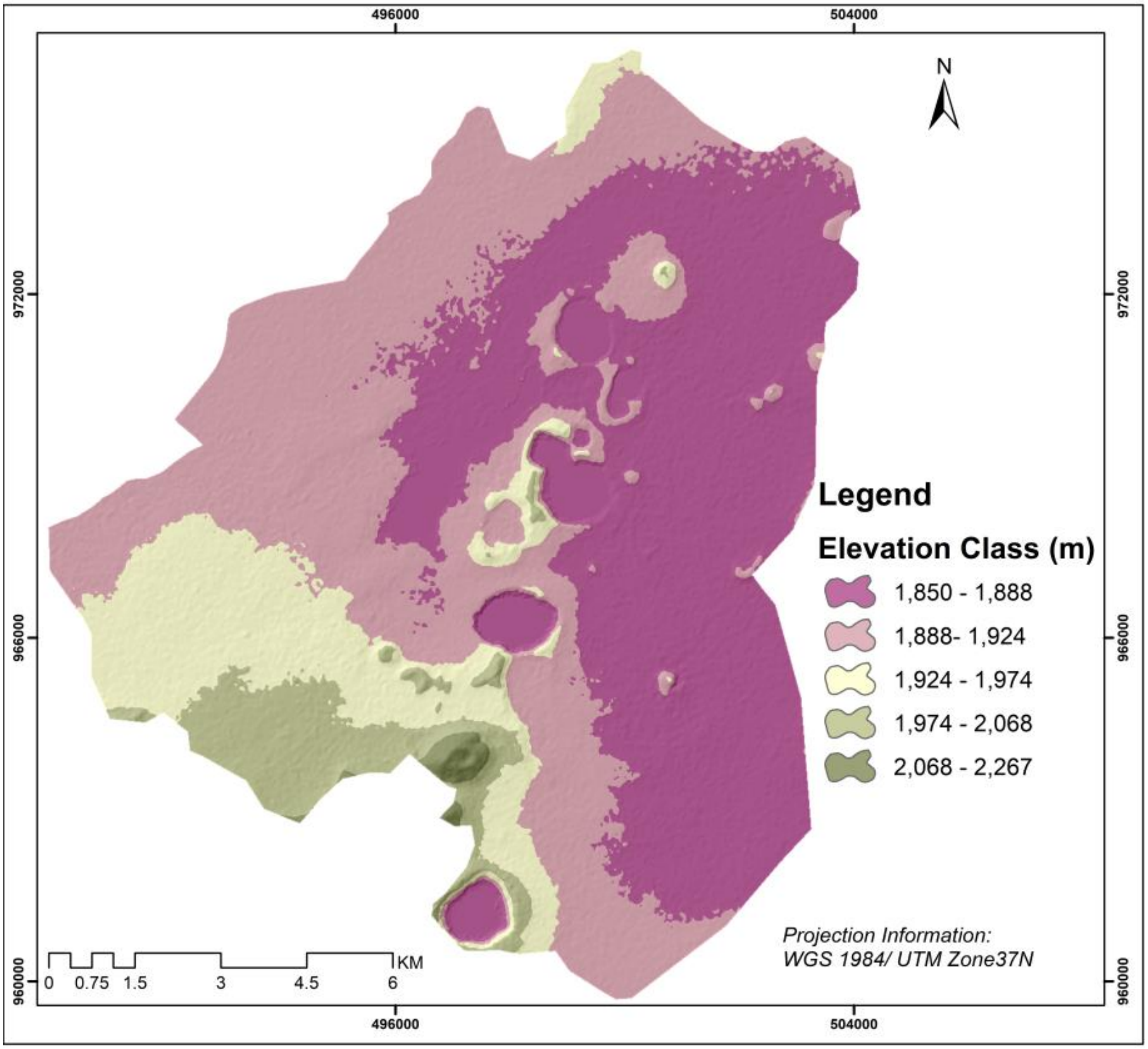

Figure 3:5 Elevation map of Bishoftu City

3.5.4 Curve Number

The flood magnitude is calculated using the flood assessment technique created by the US Natural Resources Conservation Service (NRCS), formerly known as the Soil Conservation Service (SCS). It is worth noting that there are several hydrologic methodologies utilised for flood estimation, however the SCS methodology was chosen in this research work. This approach, also known as the Curve Number (CN), uses geological information to provide a unique CN value to each location, which is then used to predict the surface runoff depth and peak discharge amplitude.

$$Q = \frac{P-0.2S^2}{P+0.8S} \quad 3.2$$

$$S = 25.4(\frac{1000}{CN}) - 10 \quad 3.3$$

$$Q_T = Q \quad 3.4$$

$$qp = quAQ \quad 3.5$$

Where Q represents the depth of direct runoff (mm), P represents the depth of precipitation for a specific return period (mm), S represents the maximum potential retention (mm), CN represents the curve number, Q_T represents the volume of runoff (m^3), A represents the basin area (Km^2), qp represents the peak discharge (m^3/s), and qu represents the unit peak discharge ($m^3/s/km^2/mm$). P was computed using statistical analysis of rainfall data to forecast the predicted rainfall depth for a certain storm of the same magnitude to occur again. Figure (3.6) depicts the curve number classes of Bishoftu City.

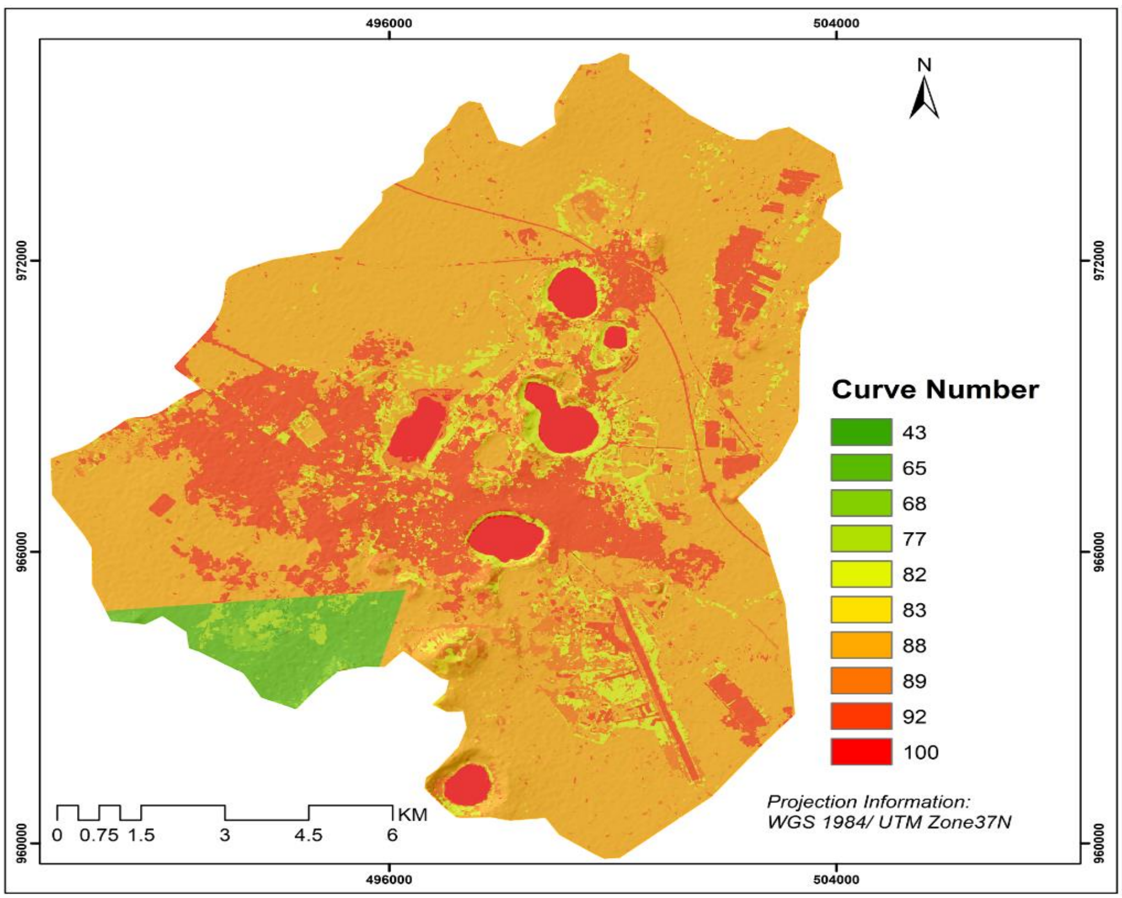

Figure 3:6 Curve Number Map of the Study Area

In this study, the curve number (CN) approach was selected since it is popular for flood assessment, requires few data, and has a modest level of complicity (Wang & Huang, 2008). Direct runoff depth is predicted by the CN technique using storm rainfall depth, land use, and soil infiltration characteristics of a catchment. To construct the land use and soil maps required for estimating flood properties, remote sensing imageries are the primary spatial data source.

3.5.5 Rainfall

Rainfall is an important aspect of developing a flood hazard map. The IDW (Inverse Distance Weight) method was used to create the rainfall map. This map developed from the thirty-two years (1990–2022) of historical rainfall data collected from meteorological stations in Bishoftu city and the surrounding six metrological stations (Akaki, Chefe Donsa, Dire Gidib, Koka Dam, Zequala, and Mojo), which helped to fill in the missing data to ensure data continuity. Furthermore, the study applied NASA Weather Satellite data (https://power.larc.nasa.gov/data-access-viewer/) for validation of the rainfall data received from the Ethiopian Metrological Agency. The IDW approach was used to provide spatial interpolation of rainfall from point data. IDW interpolation is a method of interpolation in which the sample points are weighted during interpolation so that the influence of one point on another decreases as the distance from the unknown location increases. To determine cell values, IDW interpolation employs a linearly weighted combination of a sequence of sample points. The interpolated surface was then turned into a raster layer before being classified into five groups using the equal interval approach. The reclassified rainfall was assigned a value from 1 to 5, with 1 indicating considerable influence and a very high flood rate and 5 indicating very low influence and a very low flood rate. As a result, areas with extremely high rainfall were classified as 1, while areas with very low rainfall were placed at 5. As a consequence, the raster and categorized rainfall data in Figure 3.7 are presented. The more rainfall there is, the more flood-producing runoff (Gazi et al., 2019). Figure 3.7 depicts the classification of rainfall in the study region based on its impact on floods.

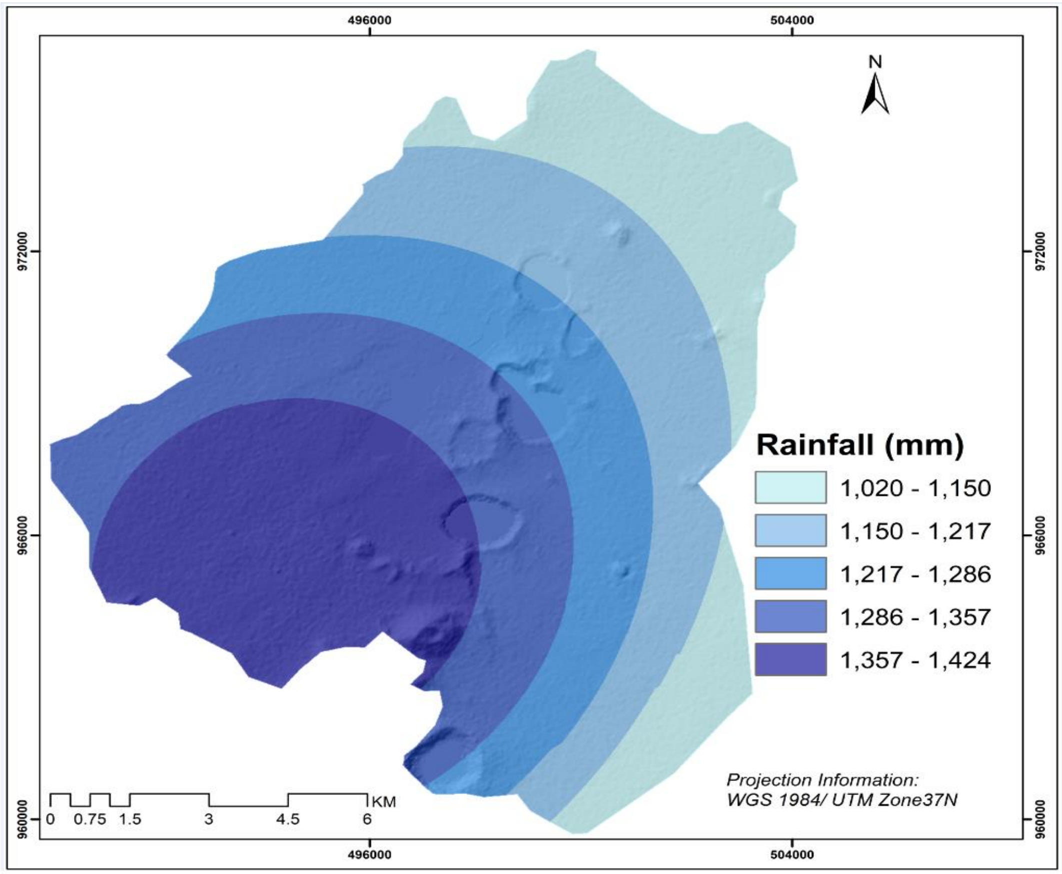

Figure 3:7 Rainfall description map.

3.5.6 Soil texture

The kind of soil has a considerable influence on the soil's infiltration rate and water-holding capacity. It may be regarded as one of the most important variables in determining flood-prone locations. Infiltration has a significant influence on the amount and availability of surface runoff produced by the rainfall-runoff process. Generally, clay soils penetrate significantly less than sandy soils (Wondim, 2016). For interpretation and analysis, the physical qualities of soil, especially textural classifications, were taken into account. Figure (3.8) depicts the principal soil textures in the research region, which include clay and sandy loam.

The hydrologic soil grouping system is used to analyze the properties of each soil category. As a result, the research area's soil group was divided into two main classes and transformed to a raster format. Furthermore, the soil raster layer group was divided into two categories. In addition, new values were allocated in the order of their flood hazard class. As shown in

Figure (3.8), soil types with a very high ability to generate a high flood rate are graded as 2, while those with a low capacity to produce a flood rate are graded as 4.

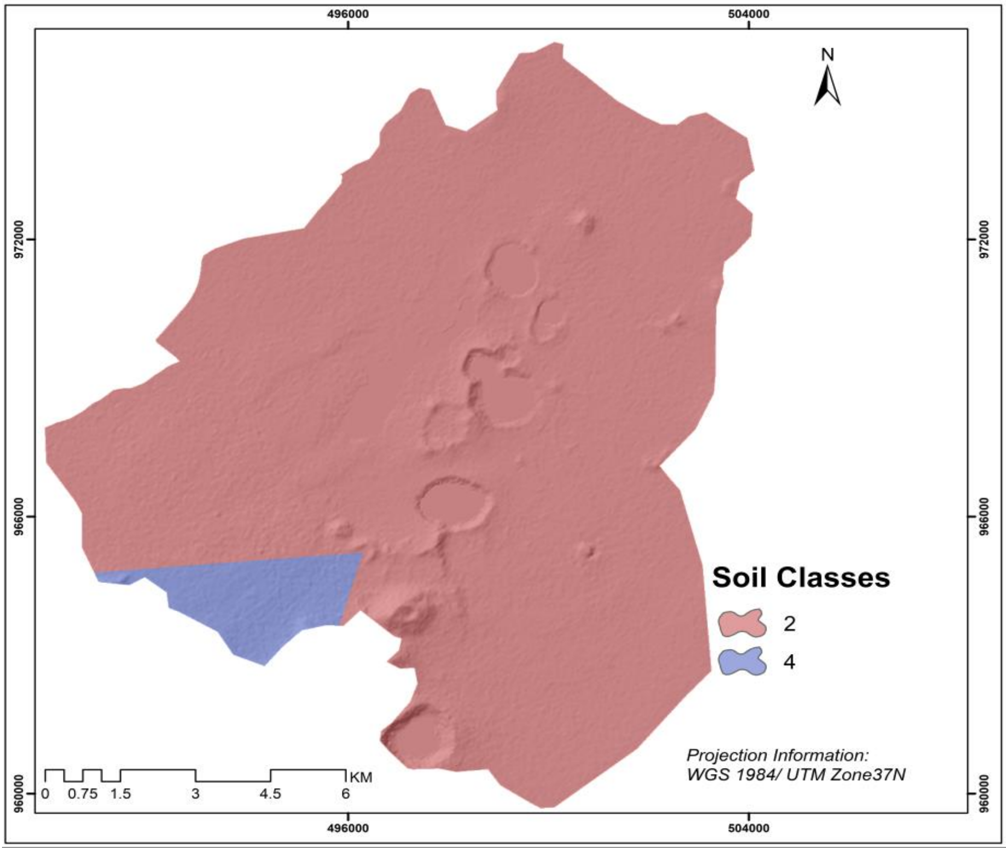

Figure 3:8 Soil Map of The Study area

3.5.7 Land use/land cover

ENVI version 5.3 was used for image classification, while ArcGIS version 10.8 was used for accuracy evaluations and image data processing, which included projection correction and map production. According to the current land use and land cover analysis; they were classified into five classes (agricultural land, built-up area, vegetation cover, bare land, and water body) and reclassified into five categories ranging from very high to very low, as shown in Figure (3.9). The land uses were then classified for the overlay analysis. As a result, the built-up area was given a very high weight, barren land was given a high weight, agricultural land was given a moderate weight, plant cover was given a low weight, and water bodies (lakes) were given a very low weight..

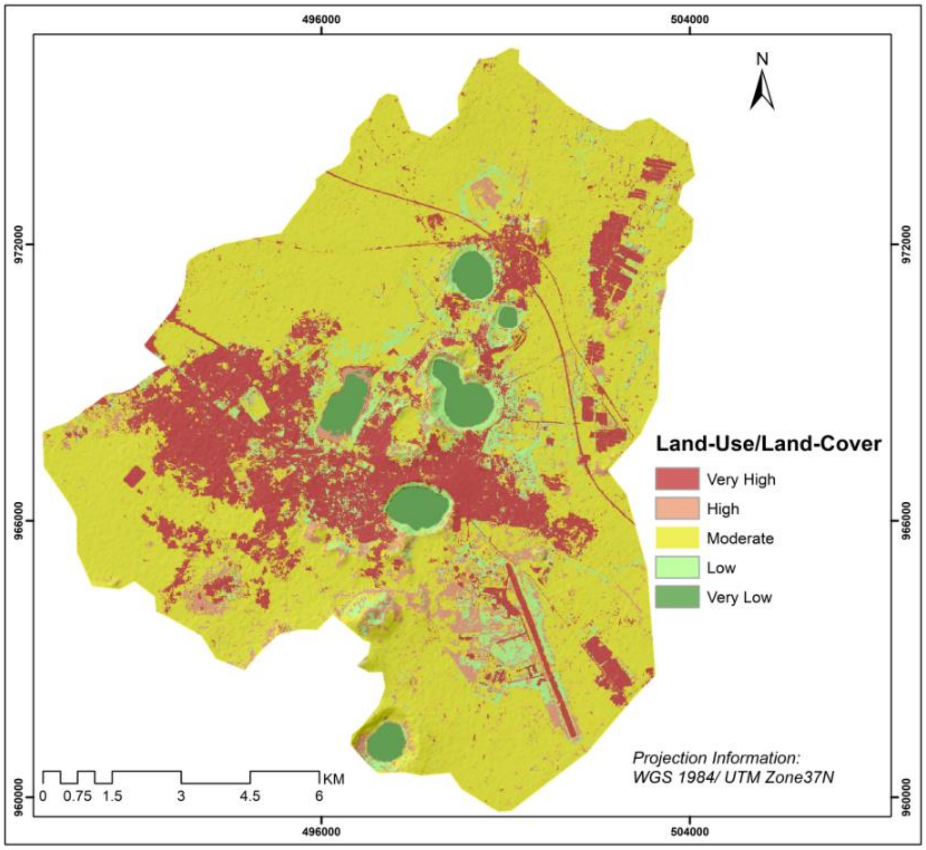

Figure 3:9 Land-use/cover Classes Maps of the Study Area.

3.6 Multi criteria Analysis

A structured decision-making tool used for managing difficult situations is multi-Criteria analysis (MCA). Sadequr (2014) defines MCA as "any deliberate and organized approach used to determine overall preferences among alternatives with the end goal of positioning them from most important to least important." MCA produces a set of weights for the various choices. The Aggregated Indices Randomization Method (AIRM), the Analytic Hierarchy Process (AHP), the Analytic Network Process (ANP), the Best Worst Method (BWM), the Characteristic Objects Method (COMET), the Choosing Advantages (CBA), and others are MCA techniques. The analytical hierarchy process (AHP) approach was chosen in this study since it is a frequently used method for flood analysis. The MCA analysis was carried out in two phases. The first phase involves determining the weights of the criteria using the Analytic Hierarchy Process (AHP), a multi-criteria decision technique. AHP builds a hierarchy of choice criteria by comparing each pair of criteria in a matrix format. The weighted scores produced by the paired comparisons represent the order of relevance of the specified criteria.

The computed weights are then used in a weighted overlay technique in the second phase to generate the flood danger map.

3.6.1 The Analytical Hierarchy Process

One of the multi criteria Analysis (MCA) methodologies used for data processing is the analytical hierarchy process (AHP). In the, Saaty, (1977) developed the Analytic Hierarchy Process as a multi-criteria decision-making technique for dealing with resource and asset allocation. Saaty developed the Pair-wise Comparison Method, which is utilised in the AHP to compute the weights or priority vectors of the selected criteria. To do the comparisons, (Saaty, 1977) requires a numerical scale that shows how many times one factor is more essential than another with which it is compared, as given in Table (3.3).

Table 3:3 Saaty's basic numerical scale

Numeric Rating	Reciprocal (decimal)	AHP Scale of Importance for comparison pair
1	1 (1.000)	Equal Importance
2	1/2(0.500)	Equally to Moderately
3	1/3(0.333)	Moderate Importance
4	1/4(0.250)	Moderately to Strong
5	1/5(0.200)	Strong Importance
6	1/6(0.167	Strongly to very strong
7	1/7 (0.143)	Very strong Importance
8	1/8 (0.125)	Very strong to extremely
9	1/9 (0.111)	Extreme Importance

To create the Analytical Hierarchy Process, a rank for each aspect was established by contacting flood-related professionals and other agricultural and environmental experts. The flood hazard analysis criteria were used to preprocess the components used as input for multi-criteria analysis. The Analytical Hierarchy Process (AHP) of Multi-criteria Analysis was used to estimate Eigen vectors for flood causative factors such as slope, drainage density, distance to the river, rainfall, elevation, soil, and land use or land cover. Individual judgments are never the same and do not always completely agree; hence, the degree of consistency achieved in matrix scaling is quantified using a Consistency Ratio (CR), which shows the likelihood that the scaling was created randomly. A CR less than or equal to 0.1 indicates that the reciprocal matrix is adequate; however, a CR greater than 0.1 indicates that the matrix should be reconsidered (Saaty, 1977). Reexamining the matrix requires discovering contradictions in the importance determinations of the criteria and revising these judgments by comparing the pair of criteria again.

The Analytical Hierarchy Process (AHP), weights, and thematic layers of each level (criteria classes) were also provided in this study, and their relative importance was calculated using Saaty's 1-9 scale. Weights have been assigned to each theme layer in relation to the other thematic levels on flood prone region definition and selection. This was done by merging relevant review literatures and expert opinion to populate a pairwise comparison matrix from which Eigenvectors and consistency ratios for each of the criteria under consideration were created (Singh et al., 2020). According to Saaty & Vargas,(1991), the reciprocal of 1 to 9 (1/1 and 1/9) suggests that one is less essential than the other. The factor weights were assessed in order to do a multi-criteria assessment of the influence on flood generation in a study region. The basic processes for establishing the indicator's weight and consistency ratio (CR) were as follows.

Step 1: Create judgement matrices (P) using pairwise comparison, where n represents the n^{th} row and m represents the m^{th} column components of the judgement matrix.

$$P = \begin{pmatrix} P_{11} & P_{12} & \cdots & P_{1n} \\ P_{21} & P_{22} & \cdots & P_{2n} \\ \vdots & \cdots & \ddots & \vdots \\ P_{n1} & P_{n2} & \cdots & P_{mn} \end{pmatrix} \quad 3.9$$

Step 2: Determine the normalised weight. The matrix is normalised in this phase by adding the integers in each column. Each column item is then divided by the column total to obtain its normalised score. Each column's total is one.

$$\mathrm{Wn} = \frac{\mathrm{GM_n}}{\sum_{n=1}^{ni} \mathrm{GM_n}} \quad 3.10$$

Where, the geometric mean of the i^{th} row of the judgments matrices is calculated as:

$$\mathrm{GM}_n = \sqrt[ni]{P_{1n}P_{2n} \ldots P_{mn}} \tag{3.11}$$

Step3. To Calculates a consistency ratio (CR) to ensure that the judgments are consistent.

Now, compute the consistency ratio and examine its value. The goal of this is to ensure that the initial preference ratings were consistent.

$$\mathrm{CR} = \frac{\mathrm{CI}}{\mathrm{RI}} \tag{3.12}$$

Consistency index (CI) is denoted as follows:

$$CI = \frac{\lambda_{max} - n_i}{n_i - 1} \tag{3.13}$$

Max is the eigenvalue of judgment matrix and it is calculated as:

$$\lambda_{max} = \sum_{n=1}^{ni} \frac{(PW)_n}{n_i w_n} \tag{3.14}$$

Where, (W) is the weight vector (column). Random index (RI) can be obtained from standard tables Saaty (1980).

The total of the weights must equal one in the Multi-criteria evaluation (MCE) technique. As a result, the weight module in QGIS employs the pairwise comparison approach to assist in the development of a collection of factor weights that add to 1 (Table 3.4). A pairwise comparison matrix compares items in terms of their relevance in relation to the specified aim, two at a time.

An individual or group assesses every conceivable pairing and inserts the rating into a pairwise comparison matrix or ratio matrix for constructing weights (Eastman, 2006). Only the lowest triangle of the matrix has to be filled in because it is symmetrical. The remaining cells are merely the lower triangle's reciprocals. After comparing all conceivable combinations of two elements, the module computes a set of weights and, more significantly, a consistency ratio. This ratio represents any discrepancies that may occur throughout the pairwise comparison procedure. The module enables repeated pairwise comparison modifications and reports the new weights and consistency ratio iterations. The factor weights and consistency ratios estimated for the factors for agricultural production in the QGIS AHP weight derivation plugin module for urban agriculture suitability study are shown in tables (3.4 and 3.5). Consistency ratio is less than the standard value (0.10). As a result, our matrix is reasonably consistent, and the estimated criteria weight will be used in the weighted overlay for further processing.

3.7 Urban Agriculture Land Suitability Analyses

3.7.1 Factors

Planning for urban agriculture and the sort of suitable site selection to be made first, as well as making decisions on them, is critical to avoiding unnecessary expenditures for a city. Several factors influence land suitability for urban agriculture. The current study considers the potential suitability of different urban agriculture sites in Bishoftu City using emerging technologies such as GIS and Remote Sensing. The weighted linear combination method was used to examine the potential sites by combining different biophysical parameters.

Six environmental land criteria were investigated in this study. As stated in Table 3.5, these are slope, drainage, elevation, soil, rainfall, and land use or land cover. The evaluation of these criteria offers information on the land's limitations for urban agricultural production. All of the aforementioned factors were taken into account for the study in order to identify potential regions for urban agricultural production, and they are plotted individually. Each criterion map depicts land appropriateness on an ordinal scale, i.e., parcels of land were assigned values of high, medium, and low suitability based on land parameters.

Table 3:4 Suitability Classes for urban agriculture.

Order	**Class**	**Description**
Suitable	Suitable	Land on which present use of the type under consideration is likely to generate benefits justifies the inputs without putting land resources at unacceptable risk or causing harm.
	Highly Suitable	Land with no substantial constraints on the long-term application of a specific use, or only minor constraints that do not considerably impair productivity or benefits and do not raise inputs over an acceptable level.
	Moderately Suitable	The land has moderately severe aggregate limitations for the sustained application of a given use; limitations that reduce productivity or benefits and increase required inputs to the extent that the overall advantage to be gained from the use, while still appealing, will be significantly less than that expected on class Highly Suitable 1 land.

	Marginally Suitable	The land has aggregate limits that are severe for long-term applications of a particular use and will lower productivity or benefits or increase necessary inputs.
Not Suitable	Not suitable	Land with characteristics that appear to limit long-term usage of the land under consideration.
	Currently not Suitable	Property having restrictions that, while surmountable in time, cannot be remedied with existing knowledge at a currently acceptable cost, and the constraints are severe enough to impede effective long-term use of the property in the given manner.
	Permanently not Suitable	Land with apparent severe constraints that interfere with any possibility of successful continued use of the land in the present manner with available knowledge.

Source: (FAO, 1993)

The GIS-based decision-making technique uses criteria maps as input data. The next stage is to merge the maps so that potential sites for urban agricultural production can be identified. The combination process is based on the standard approach for GIS-based MCDA (Malczewski, 1996). It consists of three major phases. First, the criteria maps were standardized or reclassified using the Reclassify function in Spatial Analyst. This phase is required since the criterion maps contain ordinal values (high, medium, and low) indicating the degree of land suitable for a certain criterion (criteria standardization). Second, the pairwise comparison approach was used to derive the relative relevance criteria. Once the pairwise comparison matrix is inserted in the Full Multi-criteria Evaluation plugin extension in the QGIS weight derivation module, the criterion weights are automatically produced. Third, using a weighted overlay approach to analysis, the criteria weights and standardized criterion maps were combined or aggregated. The prerequisites for urban agricultural appropriateness for Bishoftu city output are shown in Table 3.5.

Table 3.5 Urban Agriculture Land Suitability requirements

Criterion	Highly Suitable	Moderately Suitable	Marginally Suitable	Currently not Suitable	Permanently Not Suitable

Rainfall (mm)	600-800	400-600, >80	250-400	>50	
Soil (Texture)	Sandy Loam	Clay			
Slope (Degree)	0-8	8-15	15-30	>30	
Land-use/ land-cover	Agriculture land	Bare Land		Vegetation Area	*Water body, Built-up area*
Elevation (m)	1500	2500-3000	3000-3500		
Drainage Networks (m)	30-1000	100-2500	2500-4500	<30	

3.7.2 Factor/Criteria rating

Factor ratings are numerical representations of how effectively particular conditions of linked land quality fulfill each factor/criterion. Compilations of the agricultural production requirements to be included in the evaluation were developed as a first stage. In the current study, the bio-physical aspects of the location were used as suitability analysis criterion. The second stage is to decide on the factor ratings for urban agriculture, which were divided into five categories: extremely appropriate, moderately suitable, marginally suitable, presently not suitable, and permanently not suitable.

3.7.3 Criteria Standardization

Factor ratings are numerical representations of how effectively particular conditions of linked land quality fulfill each factor or criterion. Compilations of the agricultural production requirements to be included in the evaluation were developed as a first stage. In the current study, the bio-physical aspects of the location were used as a suitability analysis criterion. The second stage is to decide on the factor ratings for urban agriculture, which were divided into five categories: extremely appropriate, moderately suitable, marginally suitable, presently not suitable, and permanently not suitable.

3.7.4 Assigning Criterion weights

The goal of weighting in land suitability analysis for urban agriculture is to reflect the relevance or preference of each component in relation to the influence of other factors on agricultural productivity. The total of the weights must equal one in the Multi-criteria Evaluation (MCE) technique. As a result, the weight module in QGIS employs the pairwise comparison approach to assist in the development of a collection of factor weights that add up to 1 Table (3.8). A pairwise comparison matrix compares two components at a time in terms of their relevance in relation to the specified purpose.

A person or group assesses every conceivable pairing and inserts the rating into a pairwise comparison matrix or ratio matrix for constructing weights (Eastman, 2006). Only the lowest triangle of the matrix has to be filled in because it is symmetrical. The remaining cells are merely the lower triangle's reciprocals. After comparing all conceivable combinations of two elements, the module computes a set of weights and, more significantly, a consistency ratio. This ratio represents any discrepancies that may occur throughout the pairwise comparison procedure. The module allows for repeated pairwise comparison modifications and reports the updated weights and consistency ratio of iteration.

3.8 Estimation of Flush Flood water potential for Urban Agriculture

Assessing of the suitability of land resources alone is not enough to determine the feasibility of implementing urban agriculture practices in a particular area. It is also crucial to evaluate the availability of water resources and determine if irrigation development is feasible using various approaches. The assessment of water resources requires a comprehensive understanding of all water flows and storage systems within the considered Bishoftu city. In order to quantify the amount of water available for urban agriculture flood depth analysis is necessary.

3.8.1 Flood Depth Analysis

The flood depth was computed by detecting the flooded domain border cells on a DEM and using a polygon layer to delineate the flood extent generated using the procedures described in Cohen et al. (2017). To do this, a cell inside the flooded domain has been provided with the elevation of its nearest border cell, which is then used to determine the local water depth by subtracting this value from the surface elevation of the cell (derived from a DEM).

To conduct this, the study initially converted the hazard rater map to a polygon. Then the flood hazard polygon was converted into a polyline layer using the ArcGIS tool. The polyline layer was then transformed to a raster layer, with cells that were not equal to the polylines assigned a "No Data" value. If the flood inundation extent layer is made up of numerous polygons or has gaps within it, the borders of these will also be specified as boundary cells. This stage produces a raster of the flooded region, with all cell values equal to "No Data" save those indicating the polyline. Secondly, a new raster layer was produced using an ArcGIS Map Algebra (conditional raster calculation) expression in which cells corresponding to the boundary raster layer (from the initial Step), which are "No Data", receive the value of the underlying DEM. Thirdly, a new raster layer was computed using the Focal Statistics tool of the ArcGIS software, which calculates the values of each input cell within the identified neighborhood around it. Lastly, a raster calculation was applied using an ArcGIS Map Algebra expression to deduct the cell value of the output of the third step data (a raster layer containing the elevation of the nearest boundary cell) by the DEM value. The values of the resulting raster layer are estimated floodwater depths. The final step was smoothing the computed result to eliminate the spatial mismatches between the DEM and the flood hazard map.

3.8.2 Crop Water Requirement

In the study area, a major cash crop used for urban agriculture was determined in order to calculate the irrigation water requirements. Bishoftu metrological station was used to calculate the irrigation water requirements for each crop that was chosen. The dominant cash crops used for urban agriculture include vegetable such as tomato, potatoes and vegetables. Crop distribution in the Bishoftu city was weighted according to its profitability and productivity.

Crop water requirement is defined as the depth of water needed to meet the water loss through evapotranspiration. Crop water requirement is estimating using CROPWAT 8.0 software. It is the multiplication of reference evapotranspiration (ETo) and crop coefficient (Kc). Reference evapotranspiration (ETo) in mm is calculating by Penman-Monteith method (Penman, 1948).It can be determined using Equation (3.15).

$$\frac{0.408(Rn-G)+\gamma\frac{900}{T+273}U_2(es-ea)}{\Delta+\gamma(1+0.34U_2)} \qquad 3.15$$

Where; ETo is Reference evapotranspiration (mm/day), Rn is Net radiation at the crop surface (MJ/m2 per day), G is Soil heat flux density (MJ/m2 per day), T is Mean daily air temperature at 2 m height (°C), u2 is Wind speed at 2 m height (m/sec), es is Saturation vapour pressure (kPa), ea is Actual vapour pressure (kPa), es - ea is Saturation vapour pressure deficit (kPa), Δ is Slope of saturation vapour pressure curve at temperature T (kPa/°C) and γ is Psychometrics constant (kPa/°C).

The details of the equation are described in Allen *et al.*, (1998). ETo represents an index of climatic demand; Kc varies predominately with the specific crop characteristics and only to a limited extent with climate. This enables the transfer of standard values for Kc between locations and between climates. This has been a primary reason for the global acceptance and usefulness of the crop coefficient approach and the Kc factors developed in past studies (Allen *et al*.1998).Crop water requirement determined as a function of ETo and Crop coefficient (kc. This can be expressed in Equation 3.16

$$ETc = Kc * \mathrm{ETo} \qquad 3.16$$

Where

ETc=actual crop evapotranspiration (mm/day)

ETO=reference crop evapotranspiration (mm/day).

Kc=crop coefficient.

3.8.3 Effective rainfall

Rainfall data is required to calculate effective rainfall, for this study Dependable rainfall (80 % probability exceedance) method has been chosen for the calculation of effective rainfall. This method which is developed by FAO can be used more for designing purpose to estimate dependable rainfall.

$$ER = 0.6TR - 10 \qquad 3.17$$

This equation is valid where (TR < 70mm)

$$ER = 0.8TR - 24 \qquad 3.18$$

Equation 3.18, is valid when (TR>70 mm)

Where; ER is Effective Rainfall

TR is Total Rainfall

3.8.4 Net irrigation water requirements

Using the climate, rainfall, crop, and soil data inputs, equation (3.16) in the CropWat software 8.0 editions computed the amount of water needed for irrigation and crop growth. In the following step, the net irrigation water demand (NIWR) was determined using ETc and effective rainfall (P_{eff}).

$$NIWR = ETC - Peff \qquad 3.19$$

Where, NIWR is Net irrigation water requirement (mm)

P_{eff} is effective rainfall (mm)

ETC is Crop evapotranspiration

3.8.5 Gross irrigation water requirement

Gross irrigation water requirement can also be calculated from

$$GIWR = \frac{NIWR}{Ea} \qquad 3.20$$

Where, Ea – application efficiency

GIWR – Gross irrigation requirement (m^3 /month)

For the purposes of this study, the irrigation efficiency value was determined to be 50% of the average value within the range that was recommended by FAO.

3.9 Analytical Framework

Figure 3.2 shows the analytical framework for making decisions on flash hazard maps and developing mitigation strategies. Topography is essential for flash hazard maps and selecting suitable ones. DEM data was derived from 12.5-metre-resolution Advanced Land Observing Satellite (ALOS) PALSAR data, which commenced in October 2014. A DEM (Digital Elevation Model) helps visualize the area for various data generation tasks (drainage network, drainage density, basin area delineation, slope, etc.). The slope data and related derivations, such as elevation, were then derived using spatial analysis techniques from the Digital Elevation Model (DEM). In the Suitability modeling, FAO Soil Classification was employed.

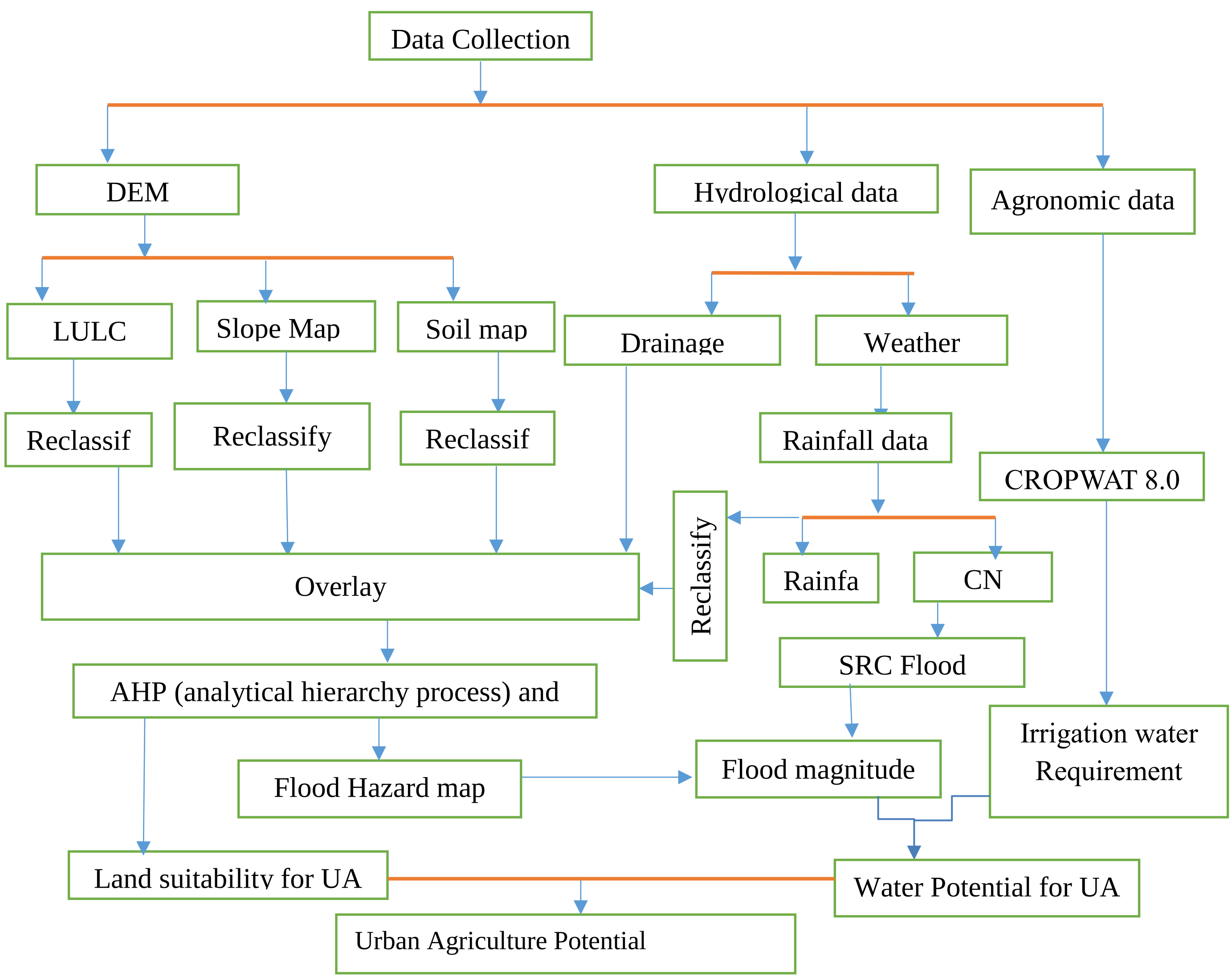

Figure 3:10 Analytical frameworks

4. RESULTS AND DISCUSSIONS

The resultant FFH map was generated from seven predictor maps and created using an integrated model with inputs from remote sensing data via the Arc GIS 10.8 analysis tool. Slope, drainage density, elevation, Curve Number, LULC, soil types, and rainfall were used as input predictors in creating the FFH map. According to Hagos et al. (2022) and similar findings with this study, high to very high food hazard zone regions were distinguished by flat areas with low slope gradient, lower height, and low drainage density, all of which are major conditioning variables for flood hazard mapping.

4.1 Land-Use/Cover Classes

4.1.1 Accuracy Assessment

The computed outcomes of the user's accuracy, the creator's accuracy, and the kappa coefficient were highlighted in Table 4.1. The table shows that the overall Kappa value is 92.7%. The classification of the water body revealed that 99.8% of the time, or nearly no pixel, was mistakenly omitted from its category. Though bare land, vegetation cover, and built-up area classes showed omissions of 11.6%, 9%, and 6.8%, respectively, Agriculture land and vegetation cover were less accurately categorized (93.3% and 94%, respectively) in the programmed classification; however, bare land showed 100% producer accuracy, showing correctly automated classification was carried out. These results revealed that the classified classes could attain the truthfulness requirements for the land cover estimation.

Table 4:1 Error matrix and accuracy level of each of Land-cover category from Sentinel-2 2023

Class Value	Built-up Area	Vegetation Cover	Water Body	Bare Land	Agricultural Land	Total	*User Accuracy (%)*
Built-up Area	466	-	-	31	3	500	93.2
Vegetation Cover	25	455	0	-	20	500	91
Water Body	-	1	499	-	-	500	99.8
Bare Land	-	28	13	447	12	500	89.4
Agricultural Land	-	-	-	13	487	500	97.4
Total	491	484	512	491	522	2500	
Producer Accuracy (%)	*94.91*	*94.01*	*97.5*	*91.04*	*93.3*		*94*
Kappa				*0.93*			

4.1.2 Land-Use/Cover Classes

The land-use and land-cover classes of Bishoftu city in 2023 are depicted in Figures (4.1) and Table (4.2), with their corresponding areas in hectares. As shown in Table 4.2, agricultural land accounted for 8788.63 ha of the entire research area, or 62.71% of the total area. This is followed by 2847.83ha of built-up area, which accounts for 20.3% of the entire area. The vegetation on the third level covers 1058.61 ha, or 7.56% of the total study area. Bare Land is the fourth LULC-class area, accounting for 885.572 ha, or 6.32% of the total area. The amount of water body cover was estimated to be around 434.564 ha, or approximately 3.1% of the research areas.

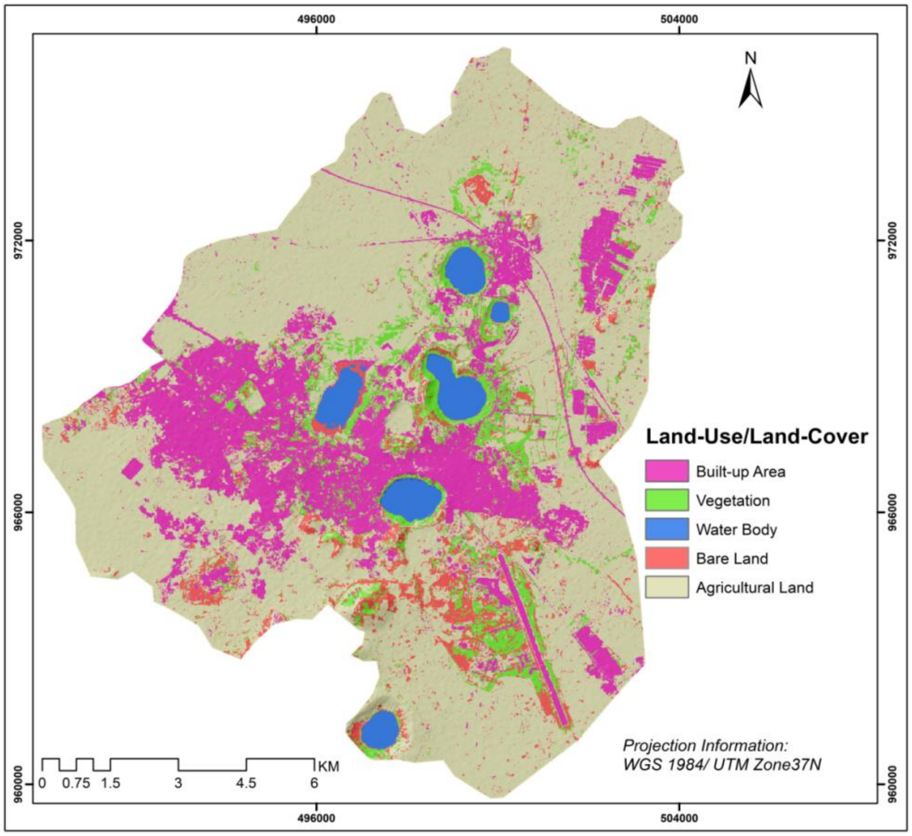

Figure 4:1 Maps illustrating the Study Area's Land Use/Cover Class

Table 4:2 Land-Use/Land-Cover Classes area in hectare

Class Name	Area (ha)	Percentage
Built-up Area	2847.83	20.3
Water Body	434.564	3.1
Vegetation	1058.61	7.56
Bare Land	885.572	6.32
Agricultural Land	8788.63	62.71
Total	14015.2	100

Moreover, the reclassified LULC (Figure 4.2, tables 4.3 and 4.4) revealed that about 20.3% (2847.8 ha) and 62.7% (8788.6 ha) of land are covered in high and low-vulnerable flood areas, respectively. Study areas that are densely inhibited, such as the most central and east parts of the city, are found to have a high to very high flash flood hazard class. According to these findings and a related study by Abdelkareem, (2017)built-up areas play a significant role in flood enhancement. Agriculture land has the lowest flash flood hazard coverage of any land use class. From this finding, we can conclude that urban agriculture provides numerous benefits to cities, one of which is flash flood, management. Urbanization without proper land use planning may increase the impermeable layer, which results in high runoff and flooding.

4.2 Slope

Slope is a particularly essential component in defining the rate of water flow and its duration. Water moves more slowly, accumulates for a longer length of time, and accumulates on larger floors, causing them to be more vulnerable to flooding than hilly places (Singh et al., 2020; Wondim, 2016). As the slope increases, the runoff also amplifies, which results in flooding. Furthermore, slopes play a significant role in the direction of flow and the degree of infiltration. Low-lying flat zones with comparatively gentle to flat slopes are more susceptible to flooding due to the runoff from high gradients. Hence, inhabitants found on such a slope were affected by flooding. Areas found in the southern part of this study area experience comparatively limited flooding when compared to the flat areas located in the western and eastern parts of the city, which have a continuous flat slope (Fig. 4.2). This finding is similar to that of Ethiopia's upper Awash River basin (Hagos et al., 2022). The outcomes of slope classes showed that more than 93.7% of the area has fallen under the very high class. Similarly, the slope is the primary element that causes people to flee from the study site. The geographical elements that induce flooding in the area clarify why the area is characterized as marshy, and the southern upper catchment of the research area is portrayed as a hilly and abandoned mountainous region where the unexpected flood originates. Bishoftu precipitation was another natural aspect studied.

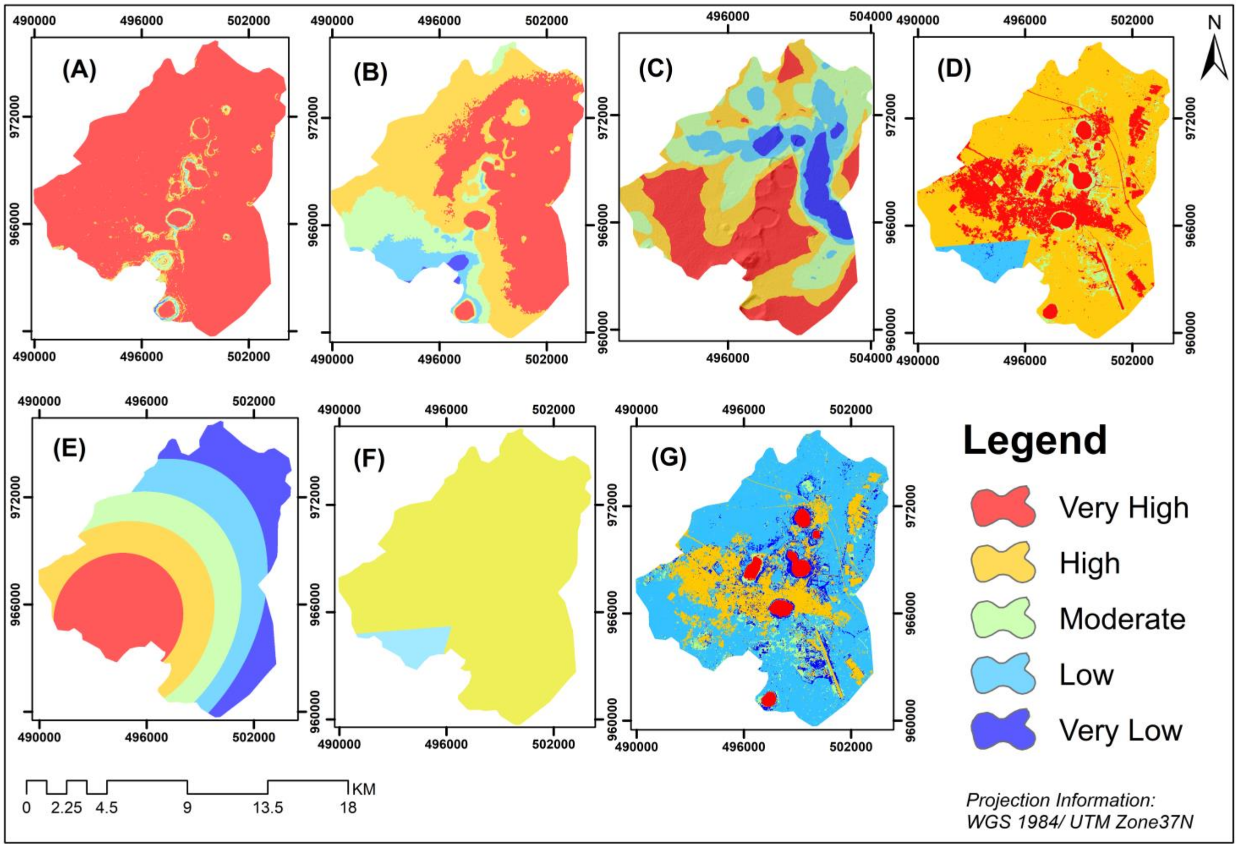

Figure 4:2 Maps of each factor for Flood Hazards Analysis (A. Slope, B. Elevation, C. Drainage, D. Curve Number, E. Rainfall, F. Soil texture and G. LULC.

Table 4:3 Classes of each flood factor with their respective area in hectare

Classes	Slope	Drainage	Elevation	Curve Number	Rainfall	Soil	LULC
Very High	13132.1	984.4	6036.9	3208.4	3167		2847.8
High	612.3	1555.2	5050.3	9138.7	2775	13371.6	434.6
Moderate	211.6	3527.1	1942.4	1014.6	2719		1058.6
Very Low	7.9	4444.4	93.5	13.0	2579		8788.6
Low	51.3	3504.0	892.2	640.5	2789	643.6	885.6
Total	**14015.2**	**14015.2**	**14015.2**	**14015.2**	**14015.2**		**14015.2**

Table 4:4 Classes of each flood factor with their respective area in percentage

FFH Classes	Slope	Drainage	Elevation	Curve Number	Rainfall	Soil	LULC
Very High	93.7	7.0	43.1	22.9	22.6		20.3
High	4.4	11.1	36.0	65.2	19.8	95.4	3.1
Moderate	1.5	25.2	13.9	7.2	19.4		7.6
Low	0.1	31.7	0.7	0.1	18.4		62.7
Very Low	0.4	25.0	6.4	And	19.9	4.6	6.3
Total	100.0	100.0	100.0	100.0	100.0	100.0	100.0

4.3 Rainfall

Heavy rainfall from surrounding highland areas is the primary cause of flooding, which causes the study area to overflow. It has been observed that the northern section of the city receives less precipitation than the eastern and southern regions. The rainfall classes revealed that about 22.6% (3168.2 ha) of Bishoftu city receives very high rainfall, followed by 19.6% (2778.6 ha) of the area receiving high rainfall per annum. Areas receiving low attention cover 18.6% (2789) of the total area of the city (Tables 4.3 and 4.4).

4.4 Drainage Density

A drainage density map was produced by calculating the total length divided by the unit area of the stream networks (Figure 4.2). These drainage density classes show that 31.7% (4444.4 ha) and 25% (3504 ha) of the study area were classified as very low and low, respectively. About 7%, 11%, and 25% of the study area fell under the very high, high, and moderate classes, respectively (Tables 4.3 and 4.4). This indicated that the area is dominated by low drainage density, which may result in flood hazards because drainage density is negatively associated with flooding(Wondim, 2016).

4.5 Soil types

According to the findings of Abdalla et al., (2015), field infiltration studies, the clear heterogeneity of soil infiltration qualities is linked to the mechanical composition and texture of the soil. Similarly, the soil class analysis in the research region (Tables 4.3 and 4.4) revealed that clay-dominated 95.4% (13371.6 ha) and sandy loam 4.6% (643.6ha) have high and low flood risk, respectively. The type of soil in a particular place may have an influence on the flood scenario since it determines infiltration potential. Soils with porous textures, such as sandy soils, absorb water readily and produce little runoff, whereas soils with less porous textures, such as clay, hold water for lengthy periods of time.

4.6 Elevation

The elevation is one of the critical indicators to understand the flash flood due to lower land areas accumulating more rainwater than areas at higher elevations, which may lead to flooding. The results of the elevation class revealed that about 13.9%, 0.7%, and 6.4% of the study areas were felled under moderate, low, and very low flash flood hazard zones, respectively (Tables 4.3 and 4.4) whereas, about 43.1% (6036.9ha) and 36% (5050.3ha) of Bishoftu city have fallen into the very high and high classes, respectively (Tables 4.3 and 4.4). The results may indicate that the elevation of the study area could contribute to flooding in Bishoftu City. A similar finding was also reported by Wondim,(2016), who stated that higher-elevation locations have decreased flood risk.

4.7 Curve number

The results of the curve number analysis of Bishoftu city fell by 30% (3208.4 ha), 65.2% (9138.7 ha), 7.2% (1014.6 ha), and 4.6% (640.5) under very high, high, moderate, and very low classes, respectively (Tables 4.3 and 4.4). The time of concentration (Tc) is greatly influenced by the curve number and surface slope. The runoff depth (Q) is inversely related to the slope and directly proportional to the curve number. Using the ArcGIS field calculation capabilities, flood hazard characteristics, including watershed storage, runoff depth, and runoff volume, was estimated. According to the CN approach equations provided in the methodology parts of this paper, the flood hazard parameters were computed.

4.8 Flash Flood Hazard (FFH)

4.8.1 Multi-Criteria Analysis

The factor weights and consistency ratios estimated for the factors for agricultural production in the QGIS AHP weight derivation plugin module for urban agriculture suitability study are shown in Tables 4.5 and 4.6. As a result, the consistency ratio (0.10) is smaller than the standard (0.10). As a result, our matrix is pretty consistent, and the estimated criteria weight will be employed in the weighted overlay for further processing. According to these findings, the slope has the greatest influence (34%) on the flash flood. And drainage density is the second most influential factor weight (24%), followed by elevation (16%) and curve number (14%), respectively (Table 4.6).

Table 4:5 Pairwise comparison of seven criterion matrix

Factors	Slope	Drainage	Elevation	Curve Number	Rainfall	Soil Texture	LULC
Slope	1						
Drainage	0.33	1					
Elevation	0.33	0.33	1				
Curve Number	0.33	0.33	0.33	1			
Rainfall	0.2	0.2	0.33	0.2	1		
Soil Texture	0.11	0.11	0.14	0.14	0.33	1	
LULC	0.11	0.11	0.14	0.11	0.2	0.33	1

Table 4:6 The Eigen vector weights of each flood factors obtained after the pairwise comparison

Factors	Normalized Weight	Influence (%)
Slope	0.34	34
Drainage	0.24	24
Elevation	0.16	16
Curve Number	0.14	14
Rainfall	0.069	6.9
Soil Texture	0.031	3.1
LULC	0.02	2
Consistent Ratio	*0.09*	

4.8.2 Flash Hazard Map

Bishoftu is one of the most susceptible regions in Ethiopia, where flood hazards have already been evaluated and mapped. To achieve the study's final goal, many methods and data processing techniques were used. Flood-triggering elements were examined and weighted using AHP methodologies. Before implementing the MCE approach, which is used to generate a final flood hazard, the consistency of the weight given for each of the criteria employed was also evaluated using the consistency ratio. It is genuinely time-consuming and expensive to build infrastructure for flood control to reduce flood damage. Flood hazard maps, on the other hand, provide information about flood-prone regions that is widely accessible to residents (Kikuchi et al., 2018). This might help people become more conscious of the hazardous location in which they reside.

Thus, flood-prone zones were assessed using seven criteria (slope, elevation, drainage density, curve number, rainfall, soil texture, and land use or cover). These factors had varying effects on the description of flood-prone areas. Each element was assigned a weight depending on its influence on flash flood production. Accordingly, Figure (4.3) and Table (4.7) present the results of the FFH map, which were divided into five zones prone to FFHs: very high, high, moderate, low, and very low, spanning 15.029%, 74.7%, 10.31%, and 0.004%, respectively.

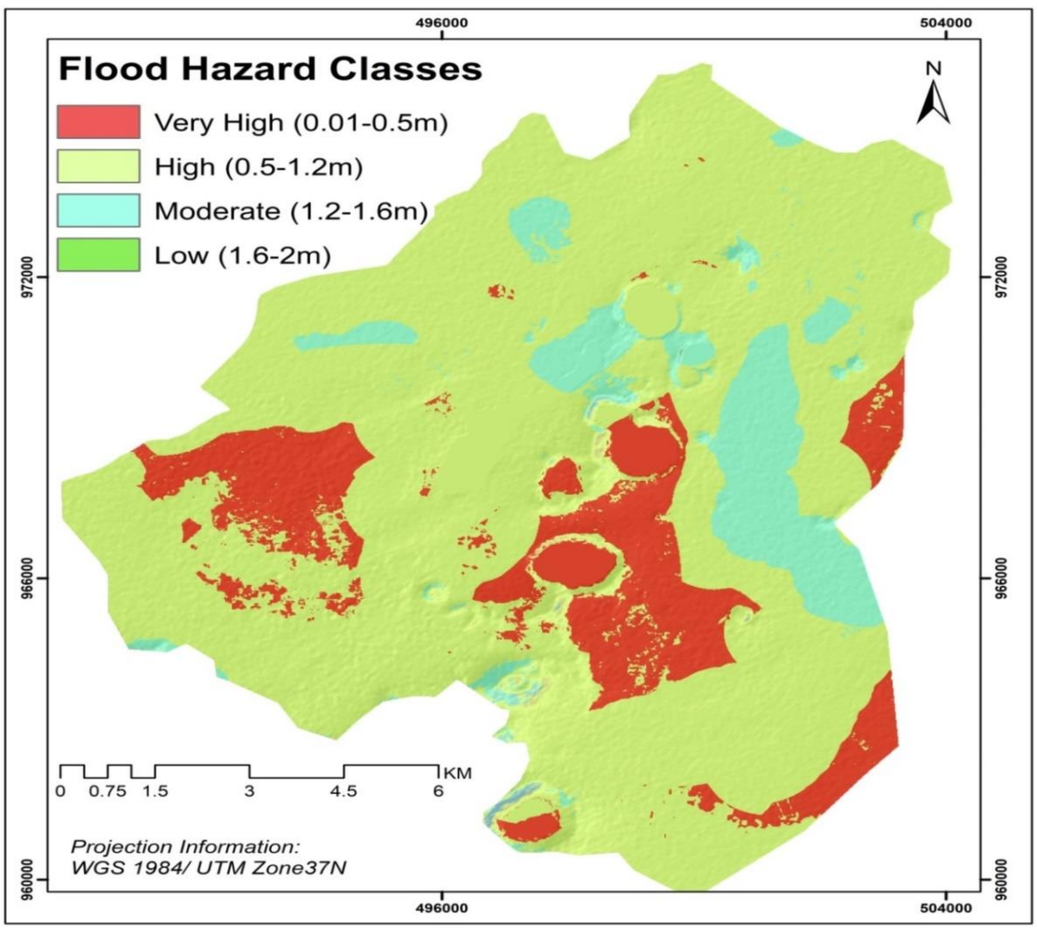

Figure 4:3 Classified Flood Hazard Map

Table 4:7 Results of Flood Hazard Area in Hectares

Hazard Level	Area (Ha)	Percent (%)
Very High	2106.36	15.03
High	10464.4	74.7
Moderate	1444.44	10.31
Low	0.523214	0.004
Total	**14015.72321**	**100%**

Furthermore, flood hazard maps, on the other hand, provide information about flood-prone regions that is widely accessible to residents (Kikuchi et al., 2018). This might help people become more conscious of the hazardous location in which they reside. Thus, flood-prone zones were assessed using seven criteria (slope, elevation, drainage density, curve number, rainfall, soil texture, and land use or cover). These factors had varying effects on the description of flood-prone areas. Each element was assigned a weight depending on its influence on flash flood production. Flood risk maps are beneficial to policymakers and responsible authorities, as well as local inhabitants, in determining appropriate flood risk reduction strategies in the research area (Dang et al., 2011). Based on the facts established by different scholars, we hope that the resulting flash flood hazard map will help the city plan flood risk management strategies.

According to the results of the analyzed datasets of drainage density, Elevation, Curve number, Rainfall, Soil type, and LULC of Bishoftu City, the area experienced FF dangers. A variety of criteria determine the occurrence of floods in a watershed, and when the defined floods in the study areas were modeled, it was found that 15.03% of Bishoftu City was at severe risk of flooding. Bishoftu City has a built-up area of roughly 20.3% in its center. As a result, flash flood threats in the central and eastern parts of Bishoftu can be caused by such built-up regions and hydrological circumstances that result in fast runoff and discharge capacity.

There was a record of probable floods in the study area if there had been yearly rainfall greater than 800mm over the past thirty years. Furthermore, the soil type in the research region is clay and sandy loam, which has a low infiltration rate and could result in runoff (Yang & Zhang, 2011).

Although slope impacts the amount of curve number and the flow rate of water over the equipotential surface, it has a substantial influence on flood threat assessment (Wondim, 2016). The flash flood hazard zones are high to extremely high in residential areas and at lower altitudes. These zones of high to very high flood danger are distinguished by flat areas with low slope degrees, lower elevation, low drainage density, and closeness to the river, all of which are essential conditioning variables for flood hazard mapping. There were extremely low to low food danger zones, which were mostly found throughout the watershed's upstream part and were distinguished by their steep slope, greater elevation, and low drainage density (Figure 4.1). This conclusion is comparable to flood hazard assessment and mapping in Ethiopia's upper Awash River basin utilizing GIS coupled with multi-criteria decision analysis (Hagos et al., 2022b); a flood vulnerability study conducted in Ethiopia's Lower Awash Sub-basin Wondim, (2016).; and the northeastern part of Bangladesh (Gazi et al., 2019).

In the study area, because of insufficient drainage facilities, which is one of the causes of flash flood hazards, after small drops of rain, the city resembles a lake that is full of flooding. The existing drainage lines, which are supposed to calm the runoff, are not properly designed due to drainage width compatibility issues, deteriorating construction materials, sedimentation of soil eroded from surrounding mountains, and poor solid waste management practices in the area, which clog the existing drainage lines. As a result, whenever it rains, residents experience flash flooding on the city's roads. Likewise, as was witnessed from the Eigenvector weights of each flood factor obtained after the pairwise comparison of flash flooding in the case site, the second factor, which is a natural factor, is Drainage density.

4.9 Urban Agriculture land suitability

Urban agriculture, as a nature-based solution, is more economical and well-made than the grey infrastructure approach to urban agriculture. In an urban area, land is set aside for urban agriculture to solve urban environmental issues such as flooding risk while simultaneously generating food for the inhabitants. So, in this study, land suitability classes for the urban agriculture region were evaluated using six criteria: land-use and land-cover classes, Slope, Rainfall, Soil, Drainage, and elevation. The research areas' urban agricultural land suitability map was the final combined resultant map created following weighted overlay analysis. This map was used to calculate different land suitability classes and their area coverage. As a result, the study found that 62.38% of the research area was extremely suitable for urban agriculture. Thus, Bishoftu is a city both comfortable to live in and easy to manage floods in by using urban agriculture as a natural flood management technique by converting flood-prone city areas to crop production. According to historical records, Adaa wereda, which includes Bishoftu city, is most commonly utilised for teff production because of its geomorphic properties, which include topographically flat land that makes it sound again.

4.9.1 Results of Each Factors

The outcome of the suitability research reveals four types of land appropriateness. These are very suitable, moderately suitable, temporarily insufficient, and permanently inadequate. Because the final appropriateness is the cumulative effect of the weighted overlay of all parameters, no site is categorized as marginally suited for the urban agriculture addressed in this study. Figure 4.2 and Table 4.4 show the results of the analyses. Thus, the results show that regions with flat to gentle slopes, agricultural land, and mean annual rainfall greater than 1000mm are biophysically more favorable for agricultural production.

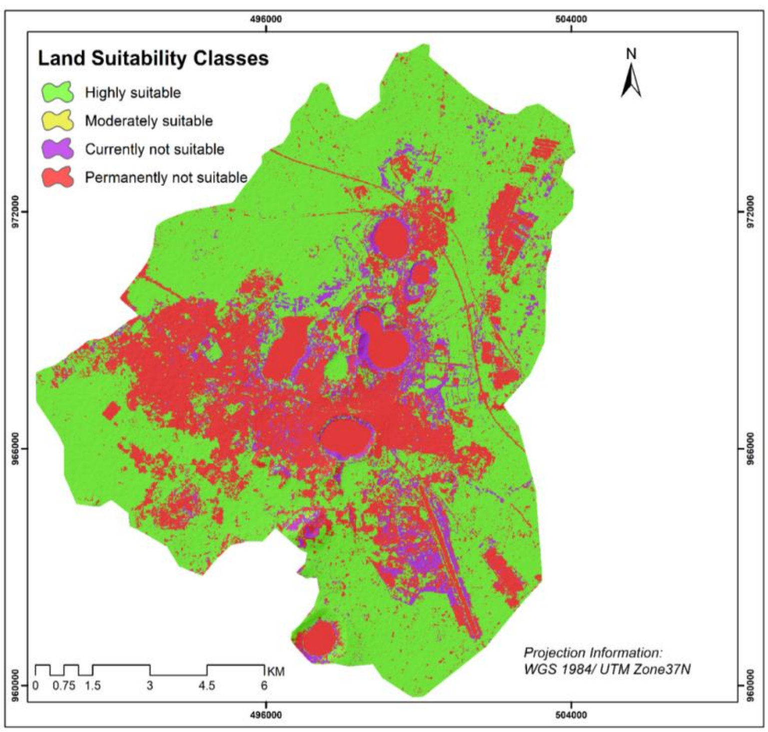

Figure 4:4 Land suitability map of Bishoftu City

Based on biophysical factors (land covers, rainfall, soil, elevation, drainage, and slope) analysis, Bishoftu City is highly suitable for agriculture production with 62.4% (8765.8 ha) of the city's land (Table 4.4 and Figure 4.4), which is more than half of the city's land. Hence, Bishoftu has a high potential for urban agriculture, which silences the flood hazard. Furthermore, the result showed that 30.2% failed under currently not suitable, 7.4% (with 62.4% (8765.8 ha) of the study area) was moderately appropriate, and 7.4% (4245.5 ha) of the study area was permanently not suitable for agriculture production.

Table 4:7 Land Suitability Classes for the Urban Agriculture

Land Suitability	Area (Ha)	Percent (%)
Highly suitable	8765.8	62.38
Moderately suitable	2.8	0.02
Currently not suitable	1037.6	7.38
Permanently not suitable	4245.5	30.21

The overall analysis results portrayed Bishoftu as ideal for urban agriculture. Based on the metropolis' various appropriateness criteria and a multi-criteria hierarchical technique, multi-objective land-use evaluation and allocation indicated the distribution of the best available agricultural fields. Thus, farm land assignment in an urban setting is required because it meets more goals (including flood risk management) than any other land-use type. According to Frantzeskaki (2019), urban agriculture is a nature-based solution that is appropriate when communities have limited economic choices for addressing environmental challenges through urban infrastructure.

Land-use/land-cover: The main factor in reducing the suitability of the urban agricultural area of the study area was a built-up area and water bodies, which cover about 23% of the city. Bare land and vegetation areas also limit the production of the urban crop. The results of the LULC suitability study revealed that a large portion of the area (62.38% (8765.5 ha)) is highly suitable for cropland. A small area of land, about 0.02 percent (2.8 ha), is moderately suitable. Out of the total city area of the district, 30.21% (4245.5ha) were permanently unsuitable (Table 4.8).

Rainfall suitability: rainfall determines the potential of the water available for plant growth. Minimal rainfall for city plant growth is not so inadequate. Usually, an annual rainfall of 500 mm is considered suitable. The findings of rainfall suitability revealed that 22.6%, 19.8%, and

57.6% of the Bishoftu city investigation fell under the highly, moderately, and marginally suitable categories for urban agriculture production (Tables 4.7).

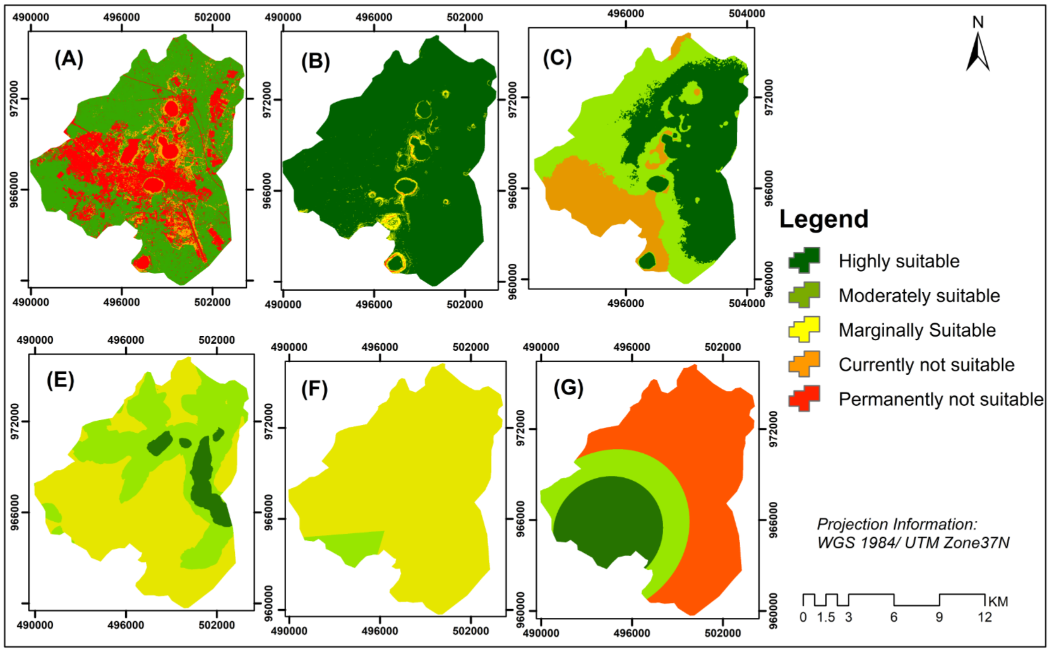

Figure 4:5 Maps of each factor for Urban Land suitability analysis (A. LULC, B. Slope, C. Drainage, D. Soil (texture), E. Drainage, F. Soil (texture), and G. Rainfall)

Slope, Soil suitability, and Elevation: These variables are usually allocated to deep and heavy soils for agriculture and soils with medium to coarse gravel. The outcomes of the slope suitability analysis revealed that a large portion of the city is relatively flat. Hence, more than 93% of the study area is highly suitable for urban agriculture, and out of the study area, about 1.4% is unsuitable for agricultural production, which may be suitable only for tourism and wildlife (Tables 4.7 and Figure 4.5). The final results of the analysis on soil suitability showed that the city in question had fewer problems regarding soil suitability for all agriculture. Thus, more than 4.6% of the area is highly suitable (Table 4.7). Furthermore, the results showed that 96.4% of the city area fell into the moderately suitable category. No area fell into the not suitable category. The analysis results for elevation stability showed that about 43%, 36%, and 21% of the study area were highly, moderately, and marginally suitable, respectively (Table 4.9).

Drainage Suitability: the results of the drainage density analysis of Bishoftu city felled under marginally suitable 82% (11475.9) while about 7% and 11.1% of the areas was highly and moderately suitable, respectively (Table 4.6).

Table 4:8 Suitability classes of each factor with their respective area coverage for Urban Agricultural land Suitability

Suitability Class	**Slope**		**Drainage**		**Elevation**		**Rainfall**		**Soil**		**LULC**	
Highly suitable	13132.1	93.7	984.1	7.0	6036.7	43.1	3168.2	22.6	644.6	4.6	8788.5	62.7
Moderately suitable	612.3	4.4	1555.2	11.1	5050.3	36.0	2777.6	19.8	13371.6	95.4	1058.5	7.6
Marginally suitable	211.6	1.5	11475.9	81.9	2928.2	20.9	8069.4	57.6				
Currently not suitable	51.3	0.4										
Permanently not suitable	7.9	0.1									4168.2	29.7
Total	**14015.2**	**100.0**	**14015.2**	**100.0**	**14015.2**	**100.0**	**14015.2**	**100.0**	**14016.2**	**100.0**	**14015.2**	**100.0**

4.9.2 Multi-Criteria Analysis for Urban Agriculture Suitability Analysis

Table 4.8 shows both factor weights as well as consistency ratios calculated for the factors for agriculture production in the QGIS **AHP** weight derivation plugin module for urban agriculture suitability analysis. Thereby, the consistency ratio is less than the standard (< 0.10). Therefore, this matrix is reasonably consistent, and the calculated criteria weight was applied for further processing in the weighted overlay. The results revealed that the LULC was the most influential factor (51%) in the flash flood. And the slope is the second most influential factor (22%), followed by rainfall (12%) and soil (7%), respectively (Table 4.9).

Table 4:9 Pairwise comparisons of six criterion matrixes

Factors	LULC	Slope	Rainfall	Soil	Drainage	Elevation	Normalized Weight	Influence (%)
LULC	1						0.51	51
Slope	0.20	1					0.22	22
Rainfall	0.14	0.33	1				0.12	12
Soil	0.11	0.20	0.33	1			0.07	7
Drainage	0.14	0.20	0.33	0.33	1		0.05	5
Elevation	0.11	0.14	0.20	0.33	0.33	1	0.03	3
Consistent Ratio						**0.09**		

4.10 Estimation of Flush Flood Water Potential for Urban Agriculture

The flood magnitude is calculated using the flood assessment technique created by the US Natural Resources Conservation Service (NRCS), formerly known as the Soil Conservation Service (SCS). This approach, also known as the Curve Number (CN), uses geological information to provide a unique CN value to each location, which is then used to predict the surface runoff depth and peak discharge amplitude.

The flood depths analysis revealed that the flood hazard covered under very high was 0 – 0.5 m, high 0.5 –1.2 m, moderate 1.2–1.6 m, and low 1.6–2 m (Figure 4.6). Based on the FFH area coverage, the areas covered by very high to high FFHs occupy approximately 89.7% of the areas surrounding the major model areas. It is worth noting that the residential area in Bishoftu City is in a very high and high flash flood zone. The FFH map was developed using a combined model with inputs from remote sensing data and the Arc GIS 10.8 processing tool. Slope, drainage density, elevation, Curve Number, LULC, soil types, and rainfall were used as input predictors in creating the FFH map.

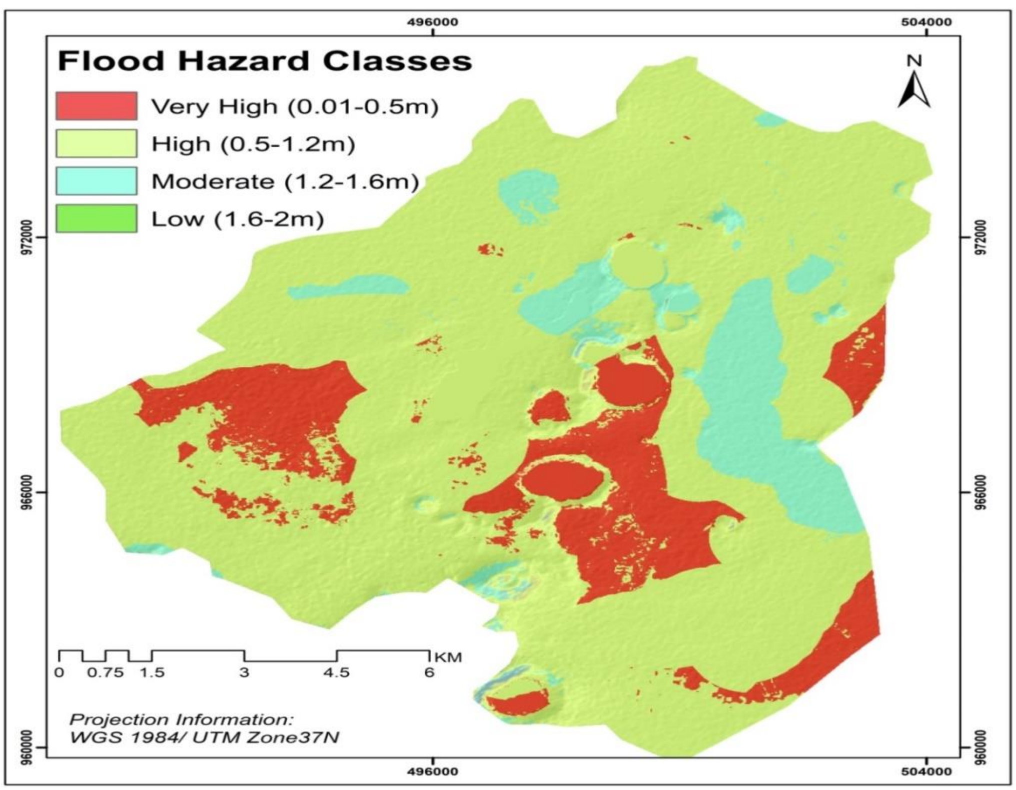

Figure 4:6 the flood depths analysis

Table 4:10 Results of Flood magnitude of Bishoftu city

FF Hazard Level	Area (Ha)	Average flood depth (mm)	Peak Flow (m^3/s)
Highly suitable	8765.6	2	8.7
Total	**8765.8**		

4.10.1 Crop Water Requirements and Irrigation Water Requirements

The term "irrigation water requirement" denotes the quantity of water that is required to supplement rainfall and sufficiently used to water crops to satisfy their water demands. This guarantees that crops obtain an adequate amount of moisture for their best possible development and productivity in areas where rainfall is inadequate. On the other hand, "crop water requirement" refers to the specified water requirements of a given crop. The amount of water needed by crops varies based on type of crop, development stage, climate, and soil properties.

Reference evapotranspiration (ETo)

The average ETo for the Bishoftu city was 4.07mm/day. It varies from 3.43 to 4.69 mm/day. The maximum ETo was in April and the minimum was recorded in the month of August.

Table 4:11 Calculated ETo values in mm/day for different month of Bishoftu city station

Months	**Jan**	**Feb**	**Mar**	**Apr**	**May**	**Jun**	**Jul**	**Aug**	**Sep**	**Oct**	**Nov**	**Dec**	**Average**
ETo(mm/day)	3.66	4.2	4.62	4.69	4.68	3.97	3.5	3.41	3.58	4.23	4.34	3.91	**4.07**

Effective rainfall (P_{eff})

Using collected average rainfall data, the CropWat program computed effective rainfall. Effective rainfall in Bishoftu city varied from 1 mm December to 145.4 mm August respectively as shown on table below.

Table 4:12 Effective rainfall of Bishoftu City in (mm)

Months	Jan	Feb	Mar	Apr	May	Jun	Jul	Aug	Sep	Oct	Nov	Dec	Total
Rainfall(mm)	8	34	52	65	73	107	178	230	99	14	3	1	864
Effective RF(mm)	7.9	32.2	47.7	58.2	64.5	88.7	127.3	145.4	83.3	13.7	3	1	672.8

4.10.2 Crop water requirements Calculations

CROPWAT 8.0 model was used to determine Crop water requirements using monthly average value of crop coefficient and ETo for each of the tomato, potato and vegetable. After the first phase of cultivation's crops was harvested, land preparation took place, and the second phase of farming and specified irrigation technique followed.

Table 4:13 Cultivation calendar for selected cash crop for urban agriculture

S/N	Crop	Area (%)	L.G.P(day)	Growing period (day)	
				Frist planting date	Frist harvesting date
1	Tomato	40	145	02/01	26/05
2	Potato	20	130	02/01	04/04
3	vegetables	40	95	04/09	06/12
	Total	100			

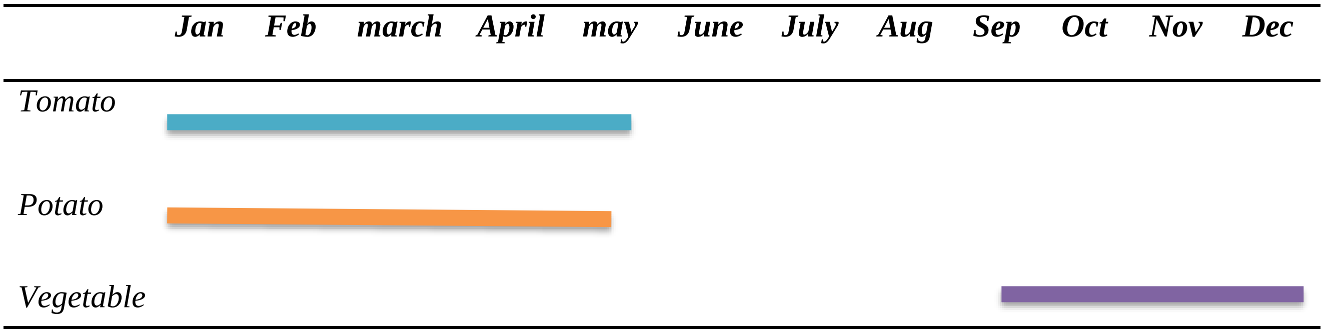

Table 4:14 Crop water requirement of selected crops for Bishoftu city (mm/month)

Months	Jan	Feb	Mar	Apr	May	Jun	Jul	Aug	Sep	Oct	Nov	Dec	**Total**
Tomato	23.8	24.8	45.1	41.5	24.5	0	0	0	0	0	0	0	159.7
Potato	19.8	30.6	46.9	37	8.8	0	0	0	0	0	0	0	143.1
Vegetables	0	0	0	0	0	0	0	0	3	44.4	52.9	11	111.3
Total (mm/month)	43.6	55.4	82.1	78.5	33.3	0	0	0	3	44.4	52.9	11	414.1

Within the Bishoftu city various crops have varying crop water requirements. Crop water requirements for selected crops, tomato, potato, and vegetables are presented in above Table for each month. From all crops tomato has highest crop water requirement which is 159.7 mm/growing period and vegetables has the lowest water requirement 111.3 mm/ growing period. Total water requirement was calculated as 414.1 mm/growing period for all crops.

Table 4.21: Command area assigned for selected crops

Crops	Area (ha)	Area (%)
Tomato	3506	40
Potato	1753	20
vegetables	3506	40
Total	**8765.8**	**100**

4.10.3 Gross Water Requirements

The estimation of gross irrigation water requirements for selected crops, i.e., tomato, potato, and vegetables, was carried out at identified potential irrigable sites from CROPWAT 8 using Kc (crop coefficient) and ETo (Reference Evapotranspiration). The gross irrigation water demand of selected crops was given in mm/month and m^3/s in table 4.15.

Table 4:15 GIWR in l/s/ha for each crop in growing period

Months	Jan	Feb	Mar	Apr	May	Jun	Jul	Aug	Sep	Oct	Nov	Dec	**Total**
Tomato	0.09	0.1	0.17	0.16	0.09	0	0	0	0	0	0	0	0.61
Potato	0.07	0.13	0.18	0.14	0.03	0	0	0	0	0	0	0	0.55
Vegetables	0	0	0	0	0	0	0	0	0.01	0.17	0.2	0.04	1.05
Total	0.16	0.23	0.35	0.3	0.12	0	0	0	0.01	0.17	0.2	0.04	2.21

4.11 Urban Agricultural potential of Bishoftu City

By comparing the irrigation needs of the land that had been determined to be suitable for urban agriculture with the available mean average flows in the Bishoftu city, the possible irrigation capacity of the study area was determined according to area division for each crop based on the approach recommended by (FAO, 1997). Gross irrigation water demand for selected cash crops such as tomato, potato and vegetables was 2.21l/s/ha. Gross irrigation water requirement for selected cash crops and suitable land was 2.21 l/s/ha, however the available water from flush flood was 8.7m^3/s, which could irrigate 8765.8 ha of urban agricultural land. But to collect such amount of water during rainy season (flush flood) its necessitates the need for storage structure in the study area to change the risk of flush flood to the opportunity and decrease the risk of flush flood in the study area.

5. CONCLUSION AND RECOMMENDATION

5.1 Conclusion

Using GIS and Remote Sensing techniques, this study attempted to build a flood inundation map and select sites appropriate for urban agriculture. On this basis, the study tried to explore in depth the primary causative elements and their relative relevance in producing flash floods. Apart from identifying and mapping flood-prone regions in the research area, promising urban agriculture sites have been identified. To fulfill the aforementioned aim, the study applied remote sensing and metrological data to map flash flood hazards (FFHs) and urban agriculture land suitability maps. The FFH model contained several evidentiary components that are commonly used in modeling flash flood dangers: slope, drainage density, elevation, Curve Number, Rainfall, soil texture, and LULC. For the land suitability model, LULC, Slope, Rainfall, Soil, Drainage, and Elevation were considered. The selected elements were developed and integrated using a GIS-based AHP paired with a multi-criteria decision analysis technique for both maps to map the flash flood-prone zones and land suitable for urban agriculture. The result of the FFH model successfully revealed four hazard zones, classifying Bishoftu City into four locations prone to FFHs, covering 15.03%, 74.7%, 10.3%, and 0.004%, respectively. Additionally, the findings of the flood depth analysis revealed that the flash hazard of the city is widely dominated by flood depths between 0.5 and 1.2 m, with a maximum flood depth of 2 m. Similarly, the resulting UALS model revealed four land suitability classes: highly suitable (62.4%), moderately suitable (0.02%), currently unsuitable (7.4%), and permanently unsuitable (7.62%), indicating that the City has a more suitable site for agricultural production. The findings of the study revealed that the residential areas in the study regions, particularly the center, are vulnerable to flood threats and that Bishoftu is appropriate for urban agriculture. In general, flood hazard mapping plays an important role in raising public awareness of flood-prone areas, lowering vulnerability to people, property, and the environment, and assisting with spatial planning decisions.

5.2 Recommendation

Based on the Research Results, the study has proposed the following recommendations, which require the participation of numerous stakeholders.

- ✓ Flash flood hazards are a live problem that occurs year in and year out. Regarding the extent of the flash flood problem and its mitigation, what I did was very minor, like fetching water from the ocean with a spoon. Thus, I recommend that further study be conducted on flood-resilient flood management options like urban agriculture.
- ✓ Planned settlement and a proper drainage system should be done. At the same time, constructions of a conservation structure on the outlet of the flood line and its use for crop production are better management options since Bishoftu is very suitable for agriculture.
- ✓ On the other hand, the lack of sufficient attention paid by the local government to flash flooding readiness prior to its occurrence was identified as a source of the worsening flooding impact on the case site. Thus, destruction of cobble roads is observed along the city, so enough attention should be given to flash floods.

REFERENCES

Abdalla, F., Al-Turki, A., & Al Amri, A. (2015). Evaluation of groundwater resources in the Southern Tihama plain, Saudi Arabia. *Arabian Journal of Geosciences*, *8*, 3299–3310.

Abdelkareem, M. (2017). Targeting flash flood potential areas using remotely sensed data and GIS techniques. *Natural Hazards*, *85*(1), 19–37.

Abebe, T., Mazzarini, F., Innocenti, F., & Manetti, P. (1998). The Yerer-Tullu Wellel volcanotectonic lineament: A transtensional structure in central Ethiopia and the associated magmatic activity. *Journal of African Earth Sciences*, *26*(1), 135–150.

Alzahrani, A. S. (2017). *Application of two-dimensional hydraulic modeling in riverine systems using HEC-RAS* [PhD Thesis]. University of Dayton.

Amaratunga, D., Sridarran, P., & Haigh, R. (2019). *Report on the Making Cities Resilient (MCR) Campaign: Comparing MCR and non-MCR cities*.

Ana Campos, G., & Ankur, N. (2020). *Building Sustainable Resilience for Sub-Saharan Africa's Urban Era*.

Argaz, A., Ouahman, B., Darkaoui, A., Bikhtar, H., Yabsa, K., & Laghzal, A. (2019). Application of remote sensing techniques and GIS-multicriteria decision analysis for groundwater potential mapping in souss watershed, Morocco. *Journal of Materials and Environmental Science*, *10*(5), 411–421.

Ayhan, E., & Kansu, O. (2012). Analysis of Image Classification Methods for Remote Sensing. *Experimental Techniques*, *36*(1), 18–25. https://doi.org/10.1111/j.1747-1567.2011.00719.x

Baker, M. (2016). Urban Agriculture is Part of the Locally Grown Food Movement. *Farm progress. Com*.

Bayissa, H. A. (2022). *The lived experiences of displayed rural farmers due to urbanization in Bishoftu City of Ethiopia* [PhD Thesis].

Benito, G., & Hudson, P. F. (2010). Flood hazards: The context of fluvial geomorphology. *Geomorphological Hazards and Disaster Prevention*, 111–128.

Bettencourt, L., & West, G. (2010). A unified theory of urban living. *Nature*, *467*(7318), 912–913.

Beven, K. J., Kirkby, M. J., Freer, J. E., & Lamb, R. (2021). A history of TOPMODEL. *Hydrology and Earth System Sciences*, *25*(2), 527–549.

Busker, T., de Moel, H., Haer, T., Schmeits, M., van den Hurk, B., Myers, K., Cirkel, D. G., & Aerts, J. (2022). Blue-green roofs with forecast-based operation to reduce the impact of weather extremes. *Journal of Environmental Management*, *301*, 113750.

Cai, Z., Page, J., & Cvetkovic, V. (2021). Urban Ecosystem Vulnerability Assessment of Support Climate-ResilientCity Development. *Urban Planning*, *3*, 227–239.

Cao, J., Wang, M., Li, Y., & Zhang, Q. (2019). Improved support vector machine classification algorithm based on adaptive feature weight updating in the Hadoop cluster environment. *PLos One*, *14*(4), e0215136.

Chakraborty, S., & Biswas, S. (2020). Application of Geographic Information System and HEC-RAS in Flood Risk Mapping of a Catchment. *Applications of Geomatics in Civil Engineering: Select Proceedings of ICGCE 2018*, 215–224.

Charleson, A., Brzev, S., Jaiswal, K., & Greene, M. (2017). Improving housing seismic safety in developing countries: The World Housing Encyclopedia. *Proc. 16th World Conference on Earthquake Engineering, Santiago, Chile*.

Cohen, S., Brakenridge, R., Kettner, A., Bates, B., Nelson, J., Mcdonald, R., Huang, Y.-F., Munasinghe, D., & Zhang, J. (2017). Estimating Floodwater Depths from Flood Inundation Maps and Topography. *JAWRA Journal of the American Water Resources Association*, *54*. https://doi.org/10.1111/1752-1688.12609

Congalton, R. G. (1991). A review of assessing the accuracy of classifications of remotely sensed data. *Remote Sensing of Environment*, *37*(1), 35–46.

Dang, N. M., Babel, M. S., & Luong, H. T. (2011). Evaluation of food risk parameters in the day river flood diversion area, Red River delta, Vietnam. *Natural Hazards*, *56*, 169–194.

Davis, R. S. (2001). Flash flood forecast and detection methods. *Severe Convective Storms*, 481–525.

De Oliveira, J. A. P., & Ahmed, A. (2021). Governance of urban agriculture in African cities: Gaps and opportunities for innovation in Accra, Ghana. *Journal of Cleaner Production*, *312*, 127730.

Deksissa, T., Trobman, H., Zendehdel, K., & Azam, H. (2021a). Integrating urban agriculture and stormwater management in a circular economy to enhance ecosystem services: Connecting the dots. *Sustainability*, *13*(15), 8293.

Deressa, T. T., Ringler, C., & Hassan, R. M. (2010). Factors affecting the choices of coping strategies for climate extremes. *The Case of Farmers in the Nile Basin of Ethiopia IFPRI Discussion Paper*, *1032*.

Du Toit, M. J., Cilliers, S. S., Dallimer, M., Goddard, M., Guenat, S., & Cornelius, S. F. (2018). Urban green infrastructure and ecosystem services in sub-Saharan Africa. *Landscape and Urban Planning*, *180*, 249–261.

Eastman, J. R. (2006). IDRISI Andes guide to GIS and image processing. *Clark University, Worcester*, *328*.

Ebissa, G., & Desta, H. (2022). Review of urban agriculture as a strategy for building a water resilient city. *City and Environment Interactions*, 100081.

Ebissa, G., Yeshitela, K., Desta, H., & Fetene, A. (2023). Urban agriculture and environmental sustainability. *Environment, Development and Sustainability*, 1–17.

Ekeu-wei, I. T., & Blackburn, G. A. (2018). Applications of open-access remotely sensed data for flood modelling and mapping in developing regions. *Hydrology*, *5*(3), 39.

Eleni, K., Ioannis, F., Alexandros, K., Emmanouil, A., & Konstantinos, N. (2011). Flood hazard assessment based on geomorphological analysis with GIS tools-The case of Laconia (Peloponnesus, Greece). *Proceedings, Symposium GIS Ostrava*, *2011*, 11p.

El-Naqa, A., & Jaber, M. (2018). Floodplain analysis using ArcGIS, HEC-GeoRAS and HEC-RAS in Attarat Um Al-Ghudran oil shale concession area, Jordan. *J. Civil Environ Eng*, *8*(5), 1–11.

Erdinata, L., Pradipta, A. G., Ngadisih, N., Setyawan, C., & Sartika, F. D. (2021). Impact of agricultural land-use change to the surface run-off: A case study of Cereng catchment area, Kulon Progo Regency, Special Region of Yogyakarta. *IOP Conference Series: Earth and Environmental Science*, *686*(1), 012030.

Erena, S. H., & Worku, H. (2019). Urban flood vulnerability assessments: The case of Dire Dawa city, Ethiopia. *Natural Hazards*, *97*, 495–516.

Ethiopia: Dire Dawa Floods - OCHA Situation Report No. 2 - Ethiopia | ReliefWeb. (2006, August 9). https://reliefweb.int/report/ethiopia/ethiopia-dire-dawa-floods-ocha-situation-report-no-2

Feyissaa, T. A., & Tufa, F. G. (2019). Floodplain Modelling of Awetu River Sub-Basin, Jimma, Oromia, Ethiopia. *J. Mater. Environ. Sci*, *10*, 1030–1042.

Frantzeskaki, N. (2019). Seven lessons for planning nature-based solutions in cities. *Environmental Science & Policy*, *93*, 101–111.

Garrison Jr, L. P., Neumann, P. J., Erickson, P., Marshall, D., & Mullins, C. D. (2007). Using real-world data for coverage and payment decisions: The ISPOR real-world data task force report. *Value in Health*, *10*(5), 326–335.

Gashaw, W., & Legesse, D. (2011). Flood hazard and risk assessment using GIS and remote sensing in Fogera Woreda, Northwest Ethiopia. *Nile River Basin: Hydrology, Climate and Water Use*, 179–206.

Gazi, M. Y., Islam, M. A., & Hossain, S. (2019). Flood-hazard mapping in a regional scale way forward to the future hazard atlas in Bangladesh. *Malaysian J. Geosci*, *3*(1), 1–11.

Gogoase, D. E. N., Armas, I., & Ionescu, C. S. (2011). Inundation maps for extreme flood events at the mouth of the Danube River. *International Journal of Geosciences*, *2*(1), 68.

Group, W. B. (2016). *The World Bank Group A to Z 2016*. World Bank Publications.

Gwam, C. U. (2010). *22. World Meteorological Organization (WMO)*. Oxford University Press.

Hagos, Y. G., Andualem, T. G., Yibeltal, M., & Mengie, M. A. (2022). Flood hazard assessment and mapping using GIS integrated with multi-criteria decision analysis in upper Awash River basin, Ethiopia. *Applied Water Science*, *12*(7), Article 7. https://doi.org/10.1007/s13201-022-01674-8

Hoeft, C. C. (2020). Incorporating updated runoff curve number technology into NRCS directives. In *Watershed Management 2020* (pp. 78–87). American Society of Civil Engineers Reston, VA.

Jha, A. K., Bloch, R., & Lamond, J. (2012). *Cities and flooding: A guide to integrated urban flood risk management for the 21st century*. World Bank Publications.

Khan, M., & Sabbir, M. (2018). *Flood hazard mapping of dharla river floodplain using HEC-RAS 1d/2d coupled model*.

Khattak, M. S., Anwar, F., Saeed, T. U., Sharif, M., Sheraz, K., & Ahmed, A. (2016). Floodplain mapping using HEC-RAS and ArcGIS: A case study of Kabul River. *Arabian Journal for Science and Engineering*, *41*, 1375–1390.

Kikuchi, H., Fukuda, A., Tsumita, N., & Takigawa, T. (2018). Dynamic Simulation of Adaptation Policy for Flood Impacts on Urban Activities: A Case Study of Khon Kaen, Thailand. *Proceedings of the International Symposium on Lowland Technology*.

Kim, M., Kidokoro, T., & Onishi, T. (2012). Peri-urbanization and its impacts on rural livelihoods in Mumbai's urban fringe. *Peri-Urbanization and Its Impacts on Rural Livelihoods in Mumbai's Urban Fringe 48th ISOCARP Congress*, 1–10.

Kumera, E., & Woldetensae, B. (2023). Special economic zones location decision and quality of life in Ethiopia: The case of Bole Lemi-1 and Eastern Industry Zone. *Geojournal*, 1–24.

Langemeyer, J., Madrid-Lopez, C., Beltran, A. M., & Mendez, G. V. (2021). Urban agriculture—A necessary pathway towards urban resilience and global sustainability? *Landscape and Urban Planning, 210*, 104055.

Legese, B., Gumi, B., & Bule Hora, E. (2020). Flooding in Ethiopia; causes, impact, and coping mechanism a review. *Int J Res Anal Rev (IJRAR)*.

Leščešen, I., & Dolinaj, D. (2019). Regional flood frequency analysis of the Pannonian Basin. *Water*, *11*(2), 193.

Li, F., Cook, S., Geballe, G. T., & Burch Jr, W. R. (2000). Rainwater harvesting agriculture: An integrated system for water management on rainfed land in China's semiarid areas. *AMBIO: A Journal of the Human Environment*, *29*(8), 477–483.

Lillesand, T., Kiefer, R. W., & Chipman, J. (2015). *Remote sensing and image interpretation*. John Wiley & Sons.

Liu, J., Guan, X., & Liu, X. (2021). Simulation and Application Research on the River System Connectivity, Considering the Flood Control and Agricultural Water Objectives. *IOP Conference Series: Earth and Environmental Science*, *768*(1), 012036.

Lucertini, G., & Di Giustino, G. (2021). Urban and peri-urban agriculture as a tool for food security and climate change mitigation and adaptation: The case of mestre. *Sustainability*, *13*(11), 5999.

Lumbroso, D. (2020). Flood risk management in Africa. *Journal of Flood Risk Management*, *13*(3).

Malczewski, J. (1996). A GIS-based approach to multiple criteria group decision-making. *International Journal of Geographical Information Systems*, *10*(8), 955–971.

Mamo, S., Berhanu, B., & Melesse, A. M. (2019). Historical flood events and hydrological extremes in Ethiopia. In *Extreme hydrology and climate variability* (pp. 379–384). Elsevier.

Marçal, D., Mesquita, G., Kallas, L. M., & Hora, K. E. R. (2021). Urban and peri-urban agriculture in Goiânia: The search for solutions to adapt cities in the context of global climate change. *Urban Climate*, *35*, 100732.

Mihalik, E. N. (2007). *Watershed characterization and runoff modeling of the Chapel Branch Creek in Orangeburg County, South Carolina* [PhD Thesis]. College of Charleston.

Miller, J. D., & Hutchins, M. (2017). The impacts of urbanisation and climate change on urban flooding and urban water quality: A review of the evidence concerning the United Kingdom. *Journal of Hydrology: Regional Studies*, *12*, 345–362.

Mountrakis, G., Im, J., & Ogole, C. (2011). ISPRS Journal of Photogrammetry and Remote Sensing Support vector machines in remote sensing: A review. *ISPRS Journal of Photogrammetry and Remote Sensing*, *66*(3), 247–259. https://doi.org/10.1016/j.isprsjprs.2010.11.001

Prinos, P., Kortenhaus, A., Swerpel, B., & Jiménez, J. A. (2008). *Review of Flood Hazard Mapping; Floodsite Report, No*. T03-07-01, 54.

Saaty, T. L. (1977). A scaling method for priorities in hierarchical structures. *Journal of Mathematical Psychology*, *15*(3), 234–281.

Saaty, T. L., & Vargas, L. G. (1991). *Prediction, projection and forecasting: Applications of the analytic hierarchy process in economics, finance, politics, games and sports*. Springer.

Shah, M. A. R., Rahman, A., & Chowdhury, S. H. (2018). Challenges for achieving sustainable flood risk management. *Journal of Flood Risk Management*, *11*, S352–S358.

Shahpari, G., Sadeghi, H., Ashena, M., & García-León, D. (2022). Drought effects on the Iranian economy: A computable general equilibrium approach. *Environment, Development and Sustainability*, *24*(3), 4110–4127.

Shao, W., Su, X., Lu, J., Liu, J., Yang, Z., Mei, C., Liu, C., & Lu, J. (2021). Urban Resilience of Shenzhen City under Climate Change. *Atmosphere*, *12*(5), 537.

Sholihah, Q., Kuncoro, W., Wahyuni, S., Suwandi, S. P., & Feditasari, E. D. (2020). The analysis of the causes of flood disasters and their impacts in the perspective of environmental law. *IOP Conference Series: Earth and Environmental Science, 437*(1), 012056.

Singh, A. P., Arya, A. K., & Singh, D. S. (2020). Morphometric analysis of Ghaghara River Basin, India, using SRTM data and GIS. *Journal of the Geological Society of India*, *95*, 169–178.

Soulis, K. X. (2021). Soil conservation service curve number (SCS-CN) Method: Current applications, remaining challenges, and future perspectives. In *Water* (Vol. 13, Issue 2, p. 192). MDPI.

Steenkamp, J., Cilliers, E. J., Cilliers, S. S., & Lategan, L. (2021). Food for thought: Addressing urban food security risks through urban agriculture. *Sustainability*, *13*(3), Article 3.

Storey, B. J., Li, M.-H., McFalls, J. A., & Yi, Y.-J. (2009). Stormwater treatment with vegetated buffers. *Texas Transportation Institute: National Cooperative Highway Research Program (NCHRP) Project*, 25–25.

Sukhwani, V., & Shaw, R. (2020). A Water-Energy-Food Nexus based Conceptual Approach for Developing Smart Urban-Rural Linkages in Nagpur Metropolitan Area, India. *IDRiM Journal*, *10*(1), 1–22.

Sur, H. S., Bhardwaj, A., & Jindal, P. K. (2001). Performance evaluation and impact assessment of a small water-harvesting structure in the Shiwalik foothills of northern India. *American Journal of Alternative Agriculture*, *16*(3), 124–130.

Tramblay, Y., Villarini, G., & Zhang, W. (2020). Observed changes in flood hazard in Africa. *Environmental Research Letters*, *15*(10), 1040b5.

van Niekerk, D., & Nemakonde, L. D. (2017). Natural hazards and their governance in Sub-Saharan Africa. In *Oxford Research Encyclopedia of Natural Hazard Science*.

Vejre, H., Jensen, F. S., & Thorsen, B. J. (2010). Demonstrating the importance of intangible ecosystem services from peri-urban landscapes. *Ecological Complexity*, *7*(3), 338–348.

Wakuma Abaya, S., Mandere, N., & Ewald, G. (2009). Floods and health in Gambella region, Ethiopia: A qualitative assessment of the strengths and weaknesses of coping mechanisms. *Global Health Action*, *2*(1), 2019.

Wang, Y., & Huang, M. B. (2008). Optimizing parameters of SCS-CN method for application on the Loess Plateau. *Bull. Soil Water Conserv*, *28*(1), 54–58.

Wondim, Y. K. (2016). Flood hazard and risk assessment using GIS and remote sensing in lower Awash sub-basin, Ethiopia. *Journal of Environment and Earth Science*, *6*(9), 69–86.

Yang, J.-L., & Zhang, G.-L. (2011). Water infiltration in urban soils and its effects on the quantity and quality of runoff. *Journal of Soils and Sediments*, *11*, 751–761.

Yousif, M., & Bubenzer, O. (2015). Geoinformatics application for assessing the potential of rainwater harvesting in arid regions. Case study: El Daba'a area, Northwestern Coast of Egypt. *Arabian Journal of Geosciences*, *8*, 9169–9191.

Zandersen, M., Oddershede, J. S., Pedersen, A. B., Nielsen, H. Ø., & Termansen, M. (2021). Nature based solutions for climate adaptation-paying farmers for flood control. *Ecological Economics*, *179*, 106705.

Zhou, Y., Han, J., Li, J., Zhou, Y., Wang, K., & Huang, Y. (2021). Building resilient cities with stringent pollution controls: A case study of robust planning of Shenzhen City's urban agriculture system. *Journal of Cleaner Production*, *311*, 127452.

Zoka, M., Psomiadis, E., & Dercas, N. (2018). The complementary use of optical and SAR data in monitoring flood events and their effects. *Proceedings*, *2*(11), 644.

APPENDIX

Appendix 1: Sample Ground truth recorded for representative land use/land cover categories.

S/No	Easting (X)	Northing (N)	Class	S/No	Easting (X)	Northing (N)	Class
1	38.99737	8.829885	Built-up Area	1251	38.96989	8.759139	Water Body
2	39.00595	8.817519	Built-up Area	1252	38.96855	8.758941	Water Body
3	39.00523	8.814711	Built-up Area	1253	38.96768	8.758723	Water Body
4	38.97135	8.810572	Built-up Area	1254	38.9683	8.758525	Water Body
5	39.0218	8.806318	Built-up Area	1255	38.96889	8.75826	Water Body
6	39.03047	8.80896	Built-up Area	1256	38.96898	8.758062	Water Body
7	39.02789	8.8078	Built-up Area	1257	38.96733	8.757652	Water Body
8	39.0281	8.806542	Built-up Area	1258	38.96761	8.757537	Water Body
9	39.03298	8.809392	Built-up Area	1259	38.98778	8.761364	Water Body
10	38.97101	8.804816	Built-up Area	1260	38.9884	8.760532	Water Body
11	38.98191	8.801857	Built-up Area	1261	38.98945	8.762612	Water Body
12	39.01665	8.803692	Built-up Area	1262	38.98895	8.762155	Water Body
13	39.02564	8.802684	Built-up Area	1263	38.9907	8.762134	Water Body
14	39.02693	8.802548	Built-up Area	1264	38.98902	8.762113	Water Body
15	38.9858	8.798914	Built-up Area	1265	38.99108	8.762098	Water Body
16	38.98707	8.797276	Built-up Area	1266	38.99084	8.761999	Water Body
17	38.99253	8.798024	Built-up Area	1267	38.98948	8.761869	Water Body
18	38.99415	8.795112	Built-up Area	1268	38.98952	8.761676	Water Body
19	39.00049	8.797083	Built-up Area	1269	38.99166	8.761619	Water Body
20	39.00106	8.795778	Built-up Area	1270	38.99257	8.761302	Water Body
21	39.01379	8.79818	Built-up Area	1271	38.98963	8.761219	Water Body
22	39.01935	8.795482	Built-up Area	1272	38.98921	8.761214	Water Body
23	39.02367	8.798737	Built-up Area	1273	38.99172	8.760974	Water Body

24	39.02319	8.797208	Built-up Area	1274	38.98941	8.760943	Water Body
25	39.0215	8.796563	Built-up Area	1275	38.99193	8.760725	Water Body
26	39.02134	8.79505	Built-up Area	1276	38.99235	8.760517	Water Body
27	38.94987	8.789424	Built-up Area	1277	38.9918	8.760449	Water Body
28	38.98771	8.793812	Built-up Area	1278	38.99116	8.760392	Water Body
29	38.99815	8.794473	Built-up Area	1279	38.99247	8.760215	Water Body
30	38.99383	8.79415	Built-up Area	1280	38.99086	8.759981	Water Body
31	38.99782	8.792653	Built-up Area	1281	38.99221	8.759903	Water Body
32	39.00317	8.794478	Built-up Area	1282	38.99043	8.75981	Water Body
33	38.99923	8.79258	Built-up Area	1283	38.99196	8.759685	Water Body
34	38.99968	8.792133	Built-up Area	1284	38.99247	8.759539	Water Body
35	39.00223	8.790713	Built-up Area	1285	38.99078	8.759435	Water Body
36	39.00023	8.79011	Built-up Area	1286	38.99193	8.759316	Water Body
37	39.0044	8.793594	Built-up Area	1287	38.99043	8.75916	Water Body
38	39.00492	8.791649	Built-up Area	1288	38.99013	8.758915	Water Body
39	39.00603	8.79063	Built-up Area	1289	38.99332	8.758842	Water Body
40	39.02011	8.794067	Built-up Area	1290	38.99261	8.758629	Water Body
41	39.01902	8.792835	Built-up Area	1291	38.9902	8.758515	Water Body
42	39.01925	8.791301	Built-up Area	1292	38.99285	8.758328	Water Body
43	39.01787	8.790136	Built-up Area	1293	38.99311	8.758255	Water Body
44	39.02076	8.794067	Built-up Area	1294	38.9924	8.757761	Water Body
45	39.02401	8.79231	Built-up Area	1295	38.99232	8.757636	Water Body
46	39.02047	8.791275	Built-up Area	1296	38.99585	8.762711	Water Body
47	39.02274	8.790214	Built-up Area	1297	38.99695	8.762488	Water Body
48	39.02607	8.790864	Built-up Area	1298	38.99416	8.762264	Water Body
49	38.97617	8.785035	Built-up Area	1299	38.9952	8.762155	Water Body
50	39.00413	8.789356	Built-up Area	1300	38.99702	8.76191	Water Body
51	39.00323	8.788436	Built-up Area	1301	38.99599	8.761749	Water Body
52	39.00252	8.787172	Built-up Area	1302	38.99376	8.761702	Water Body
53	39.00436	8.785929	Built-up Area	1303	38.99464	8.761546	Water Body

54	39.0032	8.78555	Built-up Area	1304	38.99684	8.761463	Water Body
55	38.99913	8.78414	Built-up Area	1305	38.99456	8.761068	Water Body
56	39.00542	8.78791	Built-up Area	1306	38.99488	8.760943	Water Body
57	39.00492	8.786116	Built-up Area	1307	38.99575	8.760881	Water Body
58	39.01877	8.788384	Built-up Area	1308	38.99559	8.760246	Water Body
59	39.01691	8.787286	Built-up Area	1309	38.9963	8.760038	Water Body
60	39.01863	8.785487	Built-up Area	1310	38.99457	8.760018	Water Body
61	39.01821	8.784276	Built-up Area	1311	38.99477	8.759877	Water Body
62	39.02171	8.78752	Built-up Area	1312	38.99625	8.759877	Water Body
63	39.02039	8.786891	Built-up Area	1313	38.99662	8.759643	Water Body
64	39.0247	8.785862	Built-up Area	1314	38.99484	8.75917	Water Body
65	39.02951	8.789195	Built-up Area	1315	38.99503	8.758614	Water Body
66	38.9346	8.77881	Built-up Area	1316	38.9945	8.758452	Water Body
67	38.96325	8.779247	Built-up Area	1317	38.99451	8.758166	Water Body
68	38.98336	8.779232	Built-up Area	1318	38.9946	8.75812	Water Body
69	38.99047	8.78205	Built-up Area	1319	38.96588	8.757137	Water Body
70	38.9919	8.780906	Built-up Area	1320	38.96686	8.757126	Water Body
71	38.98946	8.778982	Built-up Area	1321	38.96613	8.756679	Water Body
72	38.99949	8.783688	Built-up Area	1322	38.96547	8.755863	Water Body
73	39.00138	8.781785	Built-up Area	1323	38.96553	8.755733	Water Body
74	39.00725	8.782305	Built-up Area	1324	38.96797	8.756783	Water Body
75	39.01959	8.783163	Built-up Area	1325	38.96747	8.756201	Water Body
76	39.01925	8.780407	Built-up Area	1326	38.96751	8.755988	Water Body
77	39.01826	8.779195	Built-up Area	1327	38.97736	8.743081	Water Body
78	39.02049	8.782835	Built-up Area	1328	38.97691	8.74241	Water Body
79	38.92957	8.773626	Built-up Area	1329	38.9774	8.742	Water Body
80	38.93614	8.777833	Built-up Area	1330	38.9771	8.741641	Water Body
81	38.94138	8.774931	Built-up Area	1331	38.9825	8.745468	Water Body
82	38.95979	8.777552	Built-up Area	1332	38.98151	8.745411	Water Body
83	38.9613	8.776231	Built-up Area	1333	38.98301	8.745182	Water Body

84	38.95864	8.775077	Built-up Area	1334	38.97991	8.745047	Water Body
85	38.96691	8.777984	Built-up Area	1335	38.98	8.744854	Water Body
86	38.96305	8.776392	Built-up Area	1336	38.97958	8.744756	Water Body
87	38.98183	8.776684	Built-up Area	1337	38.97968	8.744589	Water Body
88	38.98824	8.774271	Built-up Area	1338	38.97842	8.744454	Water Body
89	38.99374	8.775087	Built-up Area	1339	38.9825	8.744215	Water Body
90	38.9961	8.777245	Built-up Area	1340	38.98204	8.744142	Water Body
91	39.00275	8.777027	Built-up Area	1341	38.97988	8.74396	Water Body
92	39.00118	8.775945	Built-up Area	1342	38.97967	8.743669	Water Body
93	39.00625	8.775103	Built-up Area	1343	38.97936	8.743638	Water Body
94	39.02135	8.778686	Built-up Area	1344	38.98239	8.743612	Water Body
95	38.93061	8.772082	Built-up Area	1345	38.97849	8.743461	Water Body
96	38.94009	8.773028	Built-up Area	1346	38.97801	8.743284	Water Body
97	38.93727	8.769898	Built-up Area	1347	38.97783	8.743138	Water Body
98	38.94012	8.768795	Built-up Area	1348	38.97908	8.743066	Water Body
99	38.94381	8.772732	Built-up Area	1349	38.97795	8.74291	Water Body
100	38.94079	8.771343	Built-up Area	1350	38.98109	8.74279	Water Body
101	38.94276	8.770693	Built-up Area	1351	38.97808	8.742488	Water Body
102	38.94103	8.769097	Built-up Area	1352	38.98151	8.742478	Water Body
103	38.9446	8.768572	Built-up Area	1353	38.97781	8.742348	Water Body
104	38.94991	8.772674	Built-up Area	1354	38.98146	8.742228	Water Body
105	38.94786	8.771541	Built-up Area	1355	38.978	8.74213	Water Body
106	38.95026	8.770646	Built-up Area	1356	38.98008	8.741875	Water Body
107	38.94598	8.769622	Built-up Area	1357	38.98054	8.741854	Water Body
108	38.94891	8.7688	Built-up Area	1358	38.97998	8.741667	Water Body
109	38.95126	8.771473	Built-up Area	1359	38.9839	8.745556	Water Body
110	38.9553	8.769185	Built-up Area	1360	38.98313	8.745447	Water Body
111	38.95671	8.772066	Built-up Area	1361	38.98472	8.744516	Water Body
112	38.95699	8.769076	Built-up Area	1362	38.9845	8.744449	Water Body